GEOLOGY AND PETROLOGY OF THE BEYPAZARI GRANITOIDS: YASSIKAYA SECTOR

A THESIS SUBMITTED TO
THE GRADUATE SCHOOL OF NATURAL AND APPLIED SCIENCES
OF
MIDDLE EAST TECHNICAL UNIVERSITY

BY

BAŞAK BİLLUR

IN PARTIAL FULFILLMENT OF THE REQUIREMENTS
FOR
THE DEGREE OF MASTER OF SCIENCE
IN
GEOLOGICAL ENGINEERING

DECEMBER, 2004

Approval of Graduate School of Natural and Applied Sciences.

Prof. Dr. Canan Özgen
Director

I certify that this thesis satifies all the requirements as a thesis for the degree of Master of Science of Geological Engineering.

Prof. Dr. Asuman G. Türkmenoğlu
Head of Department

This is to certify that we have read this thesis and that in our opinion it is fully adequate, in scope and quality, as a thesis for the degree of Master of Science of Geological Engineering.

Assoc. Prof. Dr. A. Taylan Lünel
Supervisor

Examining Comitee Members

Prof. Dr. M. Cemal Göncüoğlu	(METU, GEOE)	_____
Prof. Dr. Asuman Günal Türkmenoğlu	(METU, GEOE)	_____
Prof. Dr. Erdin Bozkurt	(METU, GEOE)	_____
Assoc. Prof. Dr. Kadir Dirik	(HU, GEOE)	_____
Assoc. Prof. Dr. A. Taylan Lünel	(METU, GEOE)	_____

I hereby declare that all information in this document has been obtained and presented in accordance with academic rules and ethical conduct. I also declare that, as required by these rules and conduct, I have fully cited and referenced all material and results that are not original to this work.

NAME, LAST NAME: Başak Billur

SIGNATURE :

ABSTRACT

GEOLOGY AND PETROLOGY OF THE BEYPAZARI GRANITOIDS: YASSIKAYA SECTOR

Billur, Başak
M.Sc., Department of Geological Engineering
Supervisor: Assoc. Prof. Dr. A. Taylan LÜNEL
December 2004, 74 pages

Beypazarı Granitoid is a low temperature and shallow-seated batholite intruded the Tepeköy metamorphic rocks of the Central Sakarya Terrane. Composition of the granitoid varies from granite to diorite. The granitoid is unconformably overlain by Palaeocene and Eocene rock units. Thus the age is probably Late Cretaceous.

The Beypazarı Granitoid comprises mafic microgranular enclaves. The granitoid mainly consists of quartz, plagioclase, orthoclase and minor amphibole, biotite, chlorite, zircon, sphene, apatite, and opaque minerals. Plagioclase shows sericitation whereas biotite and hornblende, chloritization. Holocrystalline and hypidiomorphic are characteristic textures of the granitoid.

Geochemically, the Beypazarı Granitoid is calc-alkaline, metaluminous and I-type. REE data indicate that it may have been generated from a source similar to the upper continental crust.

The trace element data of the Beypazarı Granitoid suggest a volcanic arc tectonic setting. The possible mechanism of Beypazarı Granitoid is the north-dipping subduction of Neo-Tethyan northern branch under Sakarya continent

during Late Cretaceous. The Beypazarı Granitoid may be related with Galatean volcanic arc granitoids.

Keywords: Beypazarı Granitoid, petrology, petrochemistry, volcanic arc granitoids.

ÖZ

BEYPAZARI GRANİTOYİDLERİNİN JEOLOJİSİ VE PETROLOJİSİ: YASSIKAYA BÖLÜMÜ

Billur, Başak
Yüksek Lisans, Jeoloji Mühendisliği Anabilim Dalı
Tez Yöneticisi: Doç. Dr. A. Taylan LÜNEL
Aralık 2004, 74 sayfa

Beypazarı Granitoyidi Orta Sakarya Tektonik Birliği'nde yer alan Tepeköy metamorfiklerini kesen, düşük sıcaklıktaki sığ yerleşimli batolit kütlesidir. Granitoyidin kompozisyonu granitten diorite kadar değişim gösterir. Granitoyid Paleosen ve Eosen yaşlı birimler tarafından uyumsuz olarak örtülmüştür. Buna göre, granitoyidin yaşı muhtemelen Geç Kretase'dir.

Beypazarı Granitoiyidi mafik, mikrogranüler anklavlar içerir. Granitoyid başlıca kuvars, plajiyoklas, ortoklas ve az oranda amfibol, biyotit, klorit, zirkon, sfen, apatit ve opak minerallerden oluşur. Plajiyoklaslarda serisitleşme, biyotit ve amfibolde kloritleşme görülür. Granitoyidlerde holokristalin ve hipidiyomorf bir dokular karakteristiktir.

Jeokimyasal olarak, Beypazarı Granitoyidi kalk-alkalen, metaluminus ve İ-tipindedir. Nadir toprak element verileri, granitoyidin üst kıtasal kabuğa benzer kaynaktan türediğini göstermektedir.

Beypazarı Granitoyidinin iz element verileri volkanik ark tektonik konumunu belirtmektedir. Beypazarı Granitoyidi'nin oluşmasındaki muhtemel mekanizma, İzmir-Ankara okyanusu litosferinin Sakarya mikrokıtasının altına,

kuzeye doğru dalmasıdır. Beypazarı Granitoyidleri Galatya volkanik yay granitoyidleriyle aynı olabilir.

Anahtar Kelimeler: Beypazarı Granitoyidleri, jeoloji, petroloji, petrokimya, volkanik yay granitoyidleri.

ACKNOWLEDGEMENTS

I am deeply grateful to my supervisor Assoc. Dr. Prof. A. Taylan Lünel and Prof. Dr. M. Cemal Göncüoğlu for their guidence in preparing this thesis.

I am thankful to Department of Geological Engineering for laboratory facilities.

For transportation supply from Beypazarı to study area, I am thankful to mayor of Beypazarı, Solicitor Mansur Yavaş, and driver Bahadır Boysal.

Speacial thanks to Kaan Sayıt, for his sacrificing helps during the field study.

For their hospitality, I am indebted to owners of Hacı Bostan Konağı and Ferruh Yaman, headman of Tacettin Village.

Finally, my graditutes are for my friends, Abdullah Akman, Feray Öztoprak, Füsun Erşahin, and Müge Özyıldız, my cousin Miray Törüner, my brother Emrah Billur, and my parents, Bedri Billur and especially Hale Billur for their supports and reassurances.

TABLE OF CONTENTS

	PAGE
ABSTRACT	iv
ÖZ	vi
ACKNOWLEDGEMENTS	viii
LIST OF TABLES	xi
LIST OF FIGURES	xii
ABBREVIATION	xvi
CHAPTER 1: INTRODUCTION	1
1.1. Purpose and Scope	1
1.2. Geography	1
1.3. Method of Study	3
1.4. Previous Works	3
CHAPTER 2: REGIONAL GEOLOGY	5
2.1. The Metamorphic Basement	5
2.2. Sedimentary Cover of the Granitoids	9
2.3. Granitoid	10
CHAPTER 3: GEOLOGY	13
3.1. Beypazarı Granitoid	13
3.1.1. Granitoid	15
3.1.2. Enclaves	17
3.1.3. Aplite Dykes	17
3.2. Softa Formation	17
3.2.1. Gypsiferous Mudstone	18
3.2.2. Conglomerate	18
3.3. Alluvium	18
3.4. Structure	19
3.4.1. Faults	19

3.4.2. Joints..... 20
CHAPTER 4: PETROGRAPHY OF BEYPAZARI GRANITOID..... 22
4.1. Granitoid..... 22
4.2. Enclaves..... 33
4.3. Aplite Dykes..... 33
CHAPTER 5: PETROCHEMISTRY..... 34
5.1. Analytical Methods..... 36
5.2. Rock Classification..... 37
5.3. Magmatic Evolution..... 40
5.3.1. Fractionation Process..... 40
5.3.2. Magma Mixing..... 45
5.3.3. Assimilation..... 47
5.4. Rare Earth Element Discrimination..... 48
5.5. Major Oxide Tectonic Discrimination..... 51
5.6. Trace Element Tectonic Discrimination..... 55
5.7. Spider Diagrams..... 60
5.8. Chemical Classification of Granitoids..... 62
CHAPTER 6: DISCUSSION..... 63
CHAPTER 7: CONCLUSION..... 68

REFERENCES..... 70

LIST OF TABLES

		Page
Table 4.1.	Modal analyses of rock forming minerals in the samples (volume %) ….....	23
Table 5.1.	Major oxide compositions (wt%).....	35
Table 5.2.	Trace element compositions (ppm).....	36
Table 5.3.	Rare Earth Element compositions (ppm).....	37
Table 5.4.	ORG Normalizing Values .....…….	60

LIST OF FIGURES

Figure 1.1.	Location map of the study area……..	2
Figure 2.1.	Regional geological map of the region.....	6
Figure 2.2.	Generalized stratigraphic section of Tepeköy Metamorphics.....	8
Figure 2.3.	Generalized composite stratigraphical section of Neogene deposits in the Beypazarı Basin.....	10
Figure 2.4.	Enclave.....	11
Figure 2.5.	Highly altered granitoids around joints….....	12
Figure 2.6.	The non-conformity between sedimentary units and the granitoids……	12
Figure 3.1.	The view of the non-conformity, the granitoid (G) and the Neogene deposits (ND)……...	13
Figure 3.2.	Geological map of the Yassıkaya Sector……...	14
Figure 3.3.	Aplite dyke cutting the granitoid…….	15
Figure 3.4.	A close-up view of granitoid showing a K-Feldspar megacryst (f)…….....	16
Figure 3.5.	Elliptical cross-sections of enclaves observed, north of Tacettin Village.....	17
Figure 3.6.	An agricultural field in the region……..	19
Figure 3.7.	Minor Fault cutting the aplite dyke…….	20
Figure 3.8.	Rose diagram of joints…….	20
Figure 4.1.	The sample location map of the Beypazarı Granitoid, Yassıkaya Sector.	26
Figure 4.2.	Plot of Samples on the Streckeisen (1976) Triangular QAP diagram…….	27
Figure 4.3.	Graphic texture displayed by quartz and orthoclase (Sample B1G3, 4X, XPL)…….....	28

Figure 4.4.	Orthoclase crystal (Sample B1G1, 40X, (a) PPL, (b) XPL)…….	28
Figure 4.5.	Plagioclase ((a) Sample B2G3, 4X, XPL, (b) Sample B2G2, 4X, XPL)……	29
Figure 4.6.	Pyroxene crystal (Sample B3G2, 4X, (a) PPL, (b) XPL)…	30
Figure 4.7.	Subhedral hornblende crystal, displaying rhombus (diamond)-shape, and the two sets of cleavages (56°) (Sample B1G2, 4X, XPL and PPL views)…….	30
Figure 4.8.	Subhedral biotite crystal, showing brown pleochroism (Sample B1G1, 4X, XPL)……	31
Figure 4.9.	Opaque minerals (Sample B3G4, 4X, (a) XPL, (b) PPL)…	31
Figure 4.10.	Euhedral, wedge-shaped sphene crystals showing twinning (Sample B5G3, 4X, (a) PPL, (b) XPL) …….....	32
Figure 4.11.	Well developed, euhedral, hexagonal apatite crystal and well-developed, euhedral zircon with no cleavage and very high relief. (Sample B1G1, 60X, PPL).....	32
Figure 5.1.	Na_2O+K_2O vs SiO_2 diagram.....	38
Figure 5.2.	Na_2O+K_2O vs SiO_2 diagram	38
Figure 5.3.	SiO_2 vs Zr/TiO_2 diagram	39
Figure 5.4.	Zr/TiO_2*0.0001 vs Nb/Y diagram ……..	39
Figure 5.5.	Fe_2O_3 vs SiO_2 diagram.....	40
Figure 5.6.	CaO vs SiO_2 diagram……	41
Figure 5.7.	MgO vs SiO_2 diagram……..	41
Figure 5.8.	Al_2O_3 vs SiO_2 diagram……..……	42
Figure 5.9.	K_2 O vs SiO_2 diagram……..	42
Figure 5.10.	Na_2O vs SiO_2 diagram……..……	43
Figure 5.11.	MnO vs SiO_2 diagram…….	44
Figure 5.12.	TiO_2 vs SiO_2 diagram……..	44
Figure 5.13.	P_2O_5 vs SiO_2 diagram…….…….	45
Figure 5.14.	Nb vs CaO diagram.....	46

Figure 5.15.	Sr vs CaO diagram.....	46
Figure 5.16.	Zr vs CaO diagram.....	47
Figure 5.17.	Th vs U diagram…….	48
Figure 5.18.	Condrite Normalized REE Discrimination Diagram……..	49
Figure 5.19.	Continental Crust Normalized REE Discrimination Diagram……	49
Figure 5.20.	Lower Continental Crust Normalized REE Discrimination Diagram ….....	50
Figure 5.21.	Upper Continental Crust Normalized REE Discrimination Diagram….....	50
Figure 5.22.	K_2O vs SiO_2 diagram (wt%)…….....	53
Figure 5.23.	$FeO^T/[FeO^T+MgO]$ vs SiO_2 diagram (wt%)…….....	53
Figure 5.24.	FeO^T vs MgO diagram (wt%).....	54
Figure 5.25.	(FeO^T+MgO) vs CaO wt(%) diagram.....	54
Figure 5.26.	A/(N+K) vs A/(C+N+K) diagram.....	55
Figure 5.27.	Y(ppm) vs SiO_2 (wt%) diagram.....	57
Figure 5.28.	Rb (ppm) vs SiO_2 (wt%) diagram……	57
Figure 5.29.	Nb (ppm) vs SiO_2 (wt%) diagram……	58
Figure 5.30.	Nb vs Y diagram……..	59
Figure 5.31.	Rb vs (Y+Nb) diagram.....	59
Figure 5.32.	Behaviours of incompatible elements.....	60
Figure 5.33.	Spider Diagram for ORG.....	61
Figure 5.34.	Ocean Ridge Granitoid (ORG) normalized spider diagram for Beypazarı Granitoid.....…….	61
Figure 6.1.	Terrane map of Turkey .....…….....	65
Figure 6.2.	The northward subduction of İzmir-Ankara-Erzincan Ocean under Sakarya Composite Terrane	66
Figure 6.3.	Comparison between samples of Helvacı and Bozkurt (1994) and samples of this study area.....	67

ABBREVIATION

FeO^T	Total iron as FeO
PPL	Plane Polarized Light
XPL	Cross Polarized Light

CHAPTER I

INTRODUCTION

1.1. PURPOSE AND SCOPE

Granites can form either by fractionation from mafic magma or from magma resulted by partial melting of high-grade metamorphic terrains of the lower crust. The magmatic history and source can be traced from chemistry. The aim of this study is to identify the magmatic evolution of Beypazarı Granitoids.

Due to this purpose, the 1:25000 scaled map of the Yassıkaya sector, a 30 km^2 region between Yassıkaya, Tacettin and Tahir Villages, is prepared and about 36 samples have been collected for studying them petrographically and chemically. During study of geological mapping, the main rock associations and their relative ages are examined.

At the end of this study, nature of source rocks, magmatic process involved and tectonic environment will be discussed in the frame of geotectonic evolution of Central Anatolia.

1.2. GEOGRAPHY

Beypazarı Granitoid is located in the 1/25000 scale topographic maps of Bolu subsheets [Bolu- H27-C3 and Bolu- H27-C4] in Beypazarı, Ankara (Figure 1.1).

The main topographic features in the region are ridges and valleys. The highest apex in the region is Kartan Tepe with an altitude of 1086 m, is located to the northeast of Tahir Village (Figure 1.1).

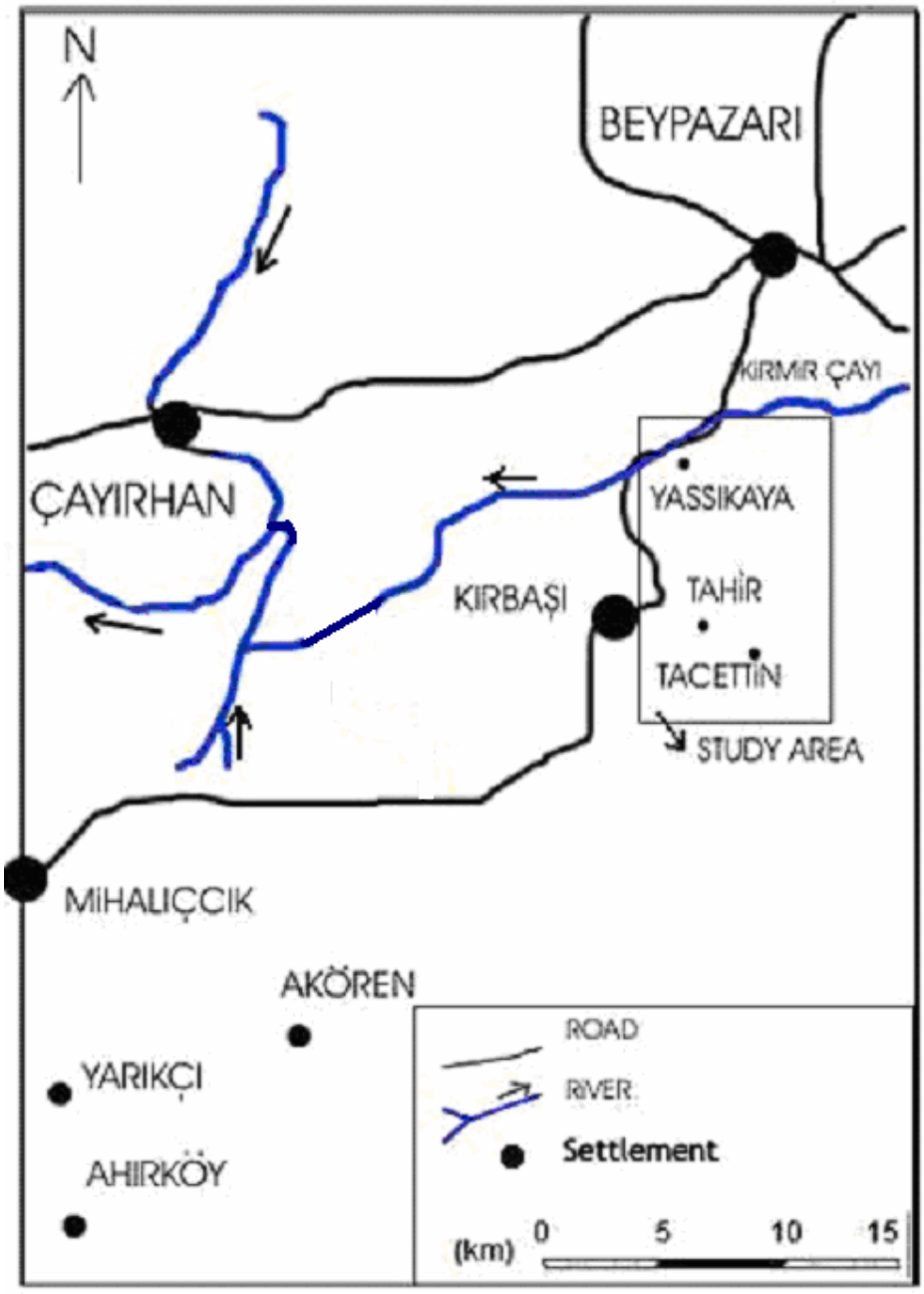

Figure 1.1. Location Map of the Study Area.

1.3. METHOD OF STUDY

Geological mapping of a region of 30 km^2 between Yassıkaya, Tacettin and Tahir villages was carried out at a scale of 1:25000 during June-July 2003. During the field work around 36 samples were collected for petrographic and chemical analyses.

Following field work, thin sections were prepared and petrographically analysed. Accordingly, 13 unaltered rock samples were selected and powdered for chemical analysis.

Modal analyses were performed on thin sections of the samples to determine the mineralogical composition. Major minerals and accessories were counted using James Swift automatic point counter.

Major oxides comprising SiO_2, Al_2O_3, total iron as Fe_2O_3, MgO, CaO, Na_2O TiO_2, MnO, and K_2O, P_2O_5, and trace and rare earth elements such as Be, Co, Cs, Ga, Hf, Nb, Rb, Sn, Sr, Ta, Th, U, V, W, Zr, Y, La, Ce, Pr, Nd, Sm, Eu, Gd, Tb, Dy, Ho, Er, Tm, Yb, Lu, Ba, Mo, Cu, Pb, Zn, Ni, As, Cd, Sb, Bi, Ag, Au, Hg, Tl, Se were analysed chemically in ACME Analytical Laboratories.

1.4. PREVIOUS WORKS

First geological investigation in the area was made by Weingart (1954). He prepared the geological map of the region on a 1/100.000 scale, named the granite-granodiorite body as “Sakarya Massive”.

Then, Van Der Meer Mohr (1956) documented the petrographic description of the granite-granodiorite intrusion and followed Weingart (1954) nomenclature.

Kalafatçıoğlu and Uysallı (1964) studied geology of the Beypazarı-Nallıhan-Seben region.

Kayakıran and Çelik (1986) made a stratigraphic correlation of the northwestern part of the region around Kirmir Çayı (Figure 2.1).

Tectonic characteristics and structural evolution of Beypazarı and Nallıhan Neogene basin is studied by Yağmurlu *et al.* (1988), and age of the granitic pluton is indicated as Permian to Paleocene.

Helvacı and Bozkurt (1991) studied the region and they presented a valuable data on the behaviour of the granite petrogenesis. They did chemical analysis and also determined an initial Sr^{87}/Sr^{86} value.

Afterwards, Yohannes (1993) studied the region. He produced a 1/25.000 scale map of 80 km^2 area at the northern part of the region. In his study, he made geological and petrochemical investigation on Beypazarı Granitoid for the purpose of petrogenesis.

Helvacı and Bozkurt (1994) made another study about geology, mineralogy and petrogenesis of Beypazarı Granite. They indicated that, metamorphic rocks of Middle Sakarya Massif are intruded by high temperature and shallow-seated batholite. This batholitic body, which has a composition ranging from granite to diorite, is called Beypazarı Granitoid. They studied the major oxide vs SiO_2 diagrams, variation diagrams of Sr, Rb and Ni versus SiO_2, and AFM diagrams and concluded that Beypazarı Granitoid was formed by anatexis of older continental crust and are shallowly intruded to the region.

Other than granites, many studies were carried out on the sedimentology and hydrogeology of the region. For example, Karadenizli (1995) studied the sedimentology of Upper Miocene-Pliocene Gypsum Series of the Beypazarı region. Özçelik (2002) studied the organic geochemical characteristics of Miocene bituminous units, north of Beypazarı.

CHAPTER II

REGIONAL GEOLOGY

The study area is located in Central Sakarya where three main Alpine tectonic units juxtapose. These are; (1) the Sömdiken Metamorphics representing the Tauride-Anatolides, (2) the Sakarya Composite Terrane and (3) the ophiolites of the İzmir-Ankara Zone (Figure 2.1) (Göncüoğlu *et al.*, 2000). The granitoid studied is within the Tepeköy Metamorphics of the Sakarya Composite Terrane.

2.1. THE METAMORPHIC BASEMENT

The basement rocks in the region are represented by the Tepeköy Metamorphic units. These metamorphics, the oldest known lithologic unit, is a member of Central Sakarya Unit of Sakarya Composite Terrane. The Central Sakarya Terrane contains three metamorphic units, the Söğüt Metamorphics, the Tepeköy Metamorphics and the Soğukkuyu Metamorphics according to Göncüoğlu *et al.* (2000).

The Söğüt Metamorphics comprises paragneisses (garnet amphibolites, silimanite-garnet gneisses, biotite-amphibole gneisses, two-mica gneisses, sillimanite-bearing staurolite schists, and mica schists and rare marble and quartzite interlayers) and granitic plutons. Many plutonic rocks of granitic-dioritic composition intrude the Söğüt Metamorphics (Yılmaz, 1981). According to Göncüoğlu *et al.* (2000), the variety of the metamorphic rock types, the presence of ophiolitic assemblages and the geochemical characteristics of the granitoids intruding them, strongly suggest a Late Palaeozoic island-arc tectonic setting for Söğüt Metamorphics.

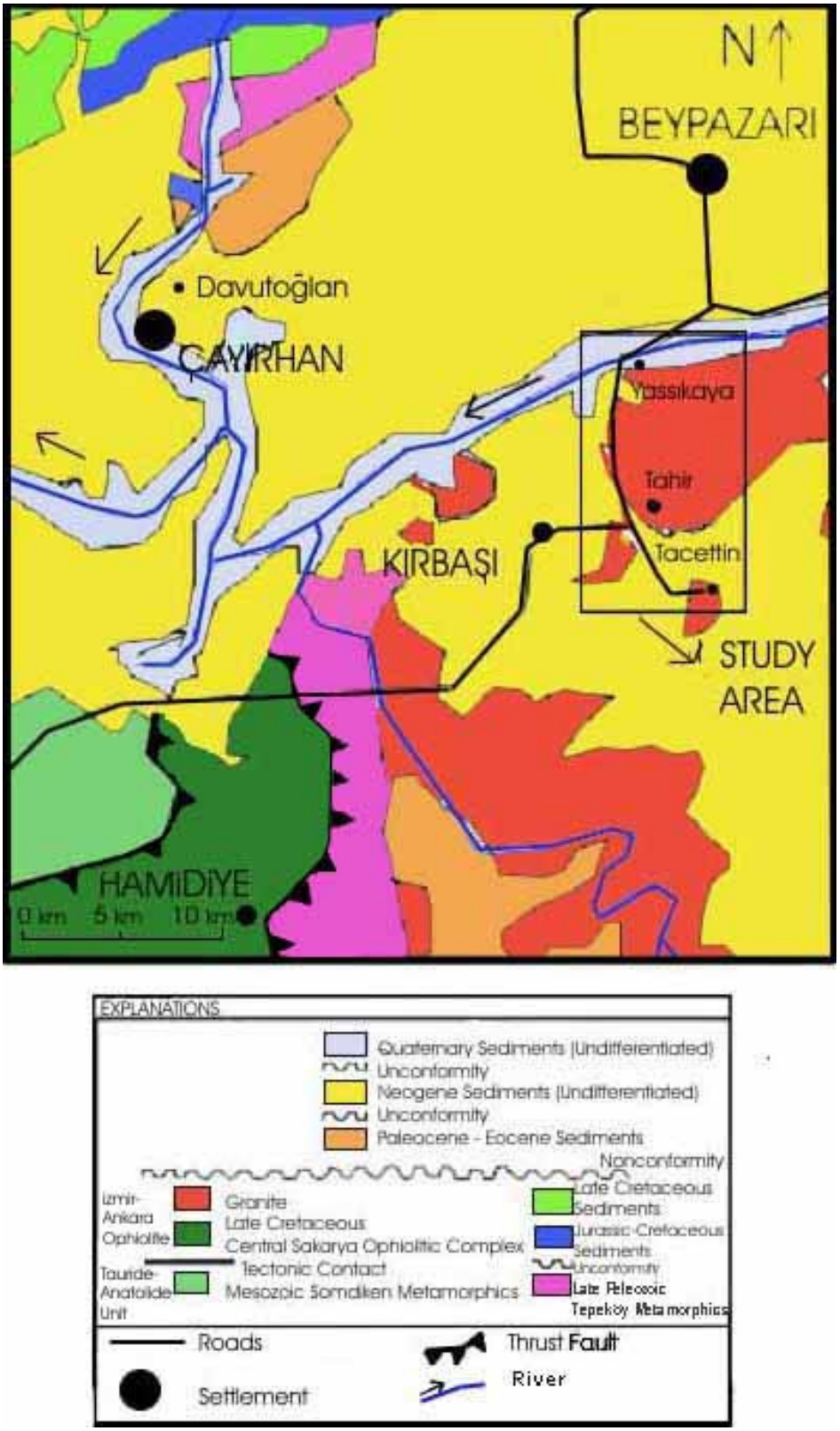

Figure 2.1. Regional Geological Map of the Region (revised after MTA, 2002).

The Tepeköy Metamorphics is composed of metabasic rocks, metatuffs, metafelsic rocks, black phyllites, metagreywackes, metasandstones and recrystallized pelagic limestone with metaradiolarite interlayers (Figure 2.2). The Tepeköy Metamorphics are unconformably overlain by basal clastic rocks of the Soğukkuyu Metamorphics containing pebbles of the Tepeköy Metamorphics. Regionally , these metamorphics correspond to the Upper Karakaya Nappe of Koçyiğit (1987).

The Soğukkuyu Metamorphics unconformably overlie the Söğüt and the Tepeköy Metamorphics according to Göncüoğlu *et al.* (2000). The rock units and their relations suggest that Soğukkuyu Metamorphics were deposited in a rifted basin, which probably opened on the accreted Söğüt and Tepeköy units and their Permian carbonate cover. The Soğukkuyu Unit corresponds to the Lower Karakaya Unit of Koçyiğit *et al.* (1991), which is mainly Late Triassic in age.

The contact relations between studied granitoid and the Tepeköy Metamorphics are not observed in the study area. However, to the northeast of the study area black slates, representatives of the Tepeköy Metamorphics are intruded by aplitic dykes. Moreover, a few km's to the southwest of the study area (Figure 2.1), a batholite (Beypazarı Granitoid of Helvacı and Bozkurt, 1994), ranging from granite to diorite intrudes metamorphic rocks, which were assigned to Triassic Karakaya Complex (MTA, 2002).

The Soğukkuyu metamorphics are disconformably overlain by Jurassic-Upper Cretaceous rocks, which occur to the northwest of the study area. They were studied by Altıner *et al.* (1991).

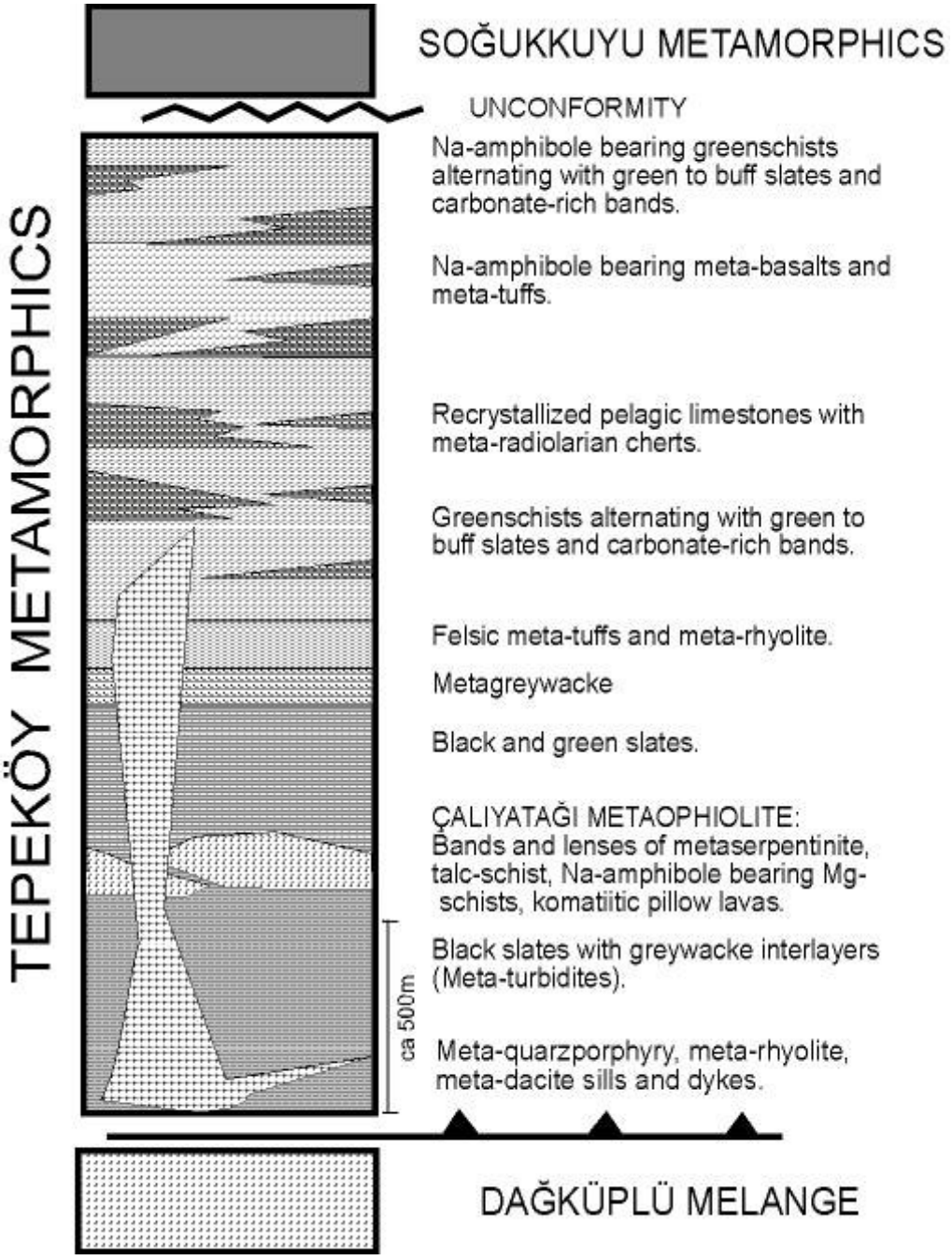

Figure 2.2. Generalized stratigraphic section of Tepeköy Metamorphics (Göncüoğlu *et al.* 2000).

2.2. SEDIMENTARY COVER OF THE GRANITOIDS

The oldest sedimentary cover of the studied granitoids is the Palaeocene-Eocene formations that exposes to the southwest of Tahir Village (Figure 2.1). Eocene sedimentary rocks are represented by Lower to Middle Eocene clastics and fossiliferous limestones (Kalafatçıoğlu and Uysallı, 1964). The basal conglomerates of this unit is dominated by granite pebbles. Thus, the intrusion age of the Beypazarı granitoid is prior to Paleocene-Early Eocene.

The Miocene sequence has been subdivided into seven sedimentary formations with eleven members and the Teke Volcanics. These sedimentary rock units are; Çoraklar, Hırka, Akpınar, Çayırhan, Bozbelen, and Kirmir formations and Sarıyar Limestone, in ascending order (Yağmurlu *et al.* 1988). Çoraklar Formation includes cross-bedded conglomerates, sandstones, mudstone and two different lignite horizons. Hırka Formation includes shale, bituminous shale, calcerous shale, dolomitic limestone, siltstone, tuffite, and trona interbeds. Akpınar Formation comprises silicified claystone, cherty limestone, and chert layers. Çayırhan Formation consists of gypsiferous claystone, mudstone, conglomerate, cross-bedded sandstone, and locally mud-cracked sandy limestone. Bozbelen Formation is made up of reddish poorly sorted conglomerate with sandstone and Kirmir Formation comprises claystone, mudstone, gypsiferous sandstone, massive gypsum horizons and thenardite-glauberite interbeds (Helvacı and Yağmurlu, 1994) (Figure 2.3).

Separation has been made certain localities between Jurassic and Lower Cretaceous limestones (Kalafatçıoğlu and Uysallı, 1964). According to Altıner *et al.*, (1991) these limestones contain capionellids, radiolaria, nannoconids *Zoophycus*, aptychi and belemnites, and they are named as Soğukçam Limestone.

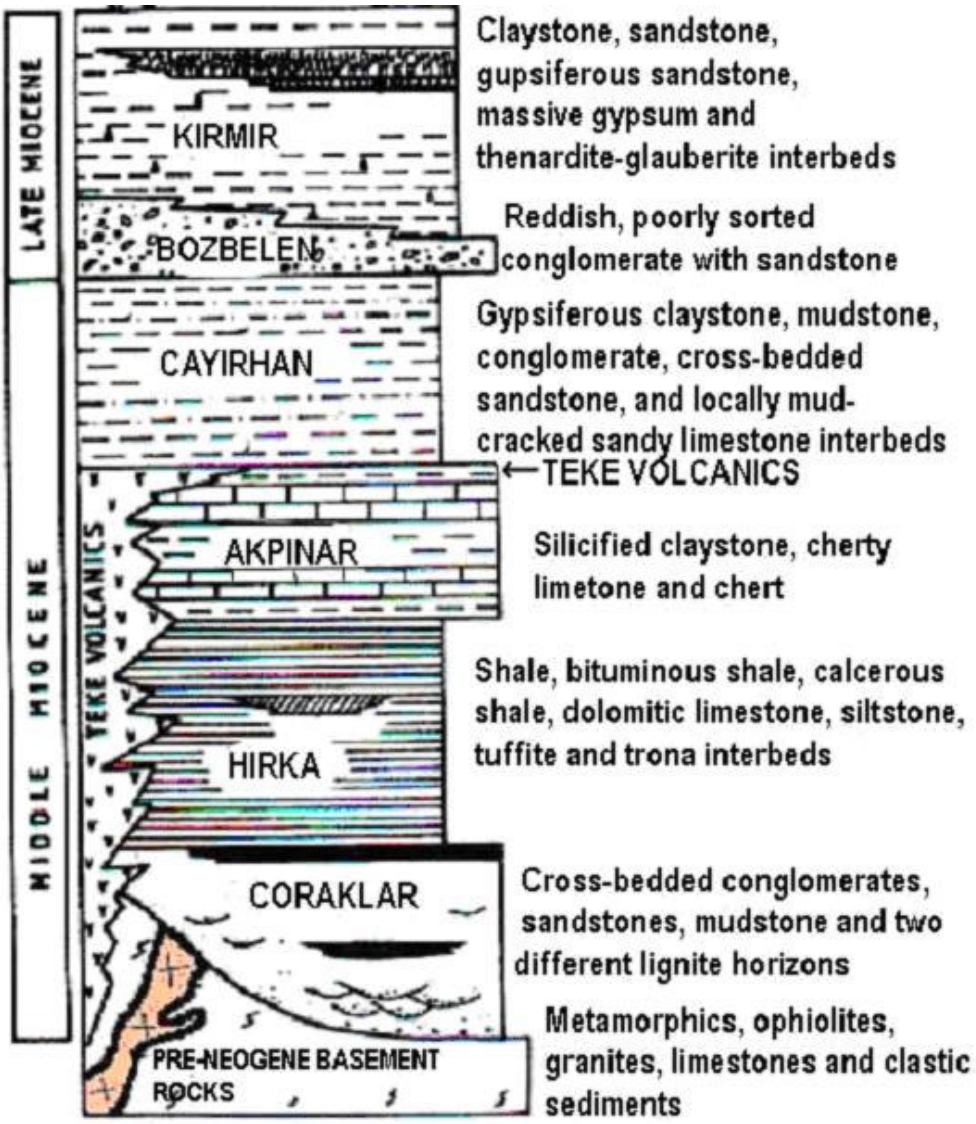

Figure 2.3. Generalized composite stratigraphical section of Neogene deposits in the Beypazarı Basin (Helvacı and Yağmurlu, 1994).

2.3. GRANITOID

In the study area, the boundaries between the granitoid and host rocks are not observed. To the south, outside the study area, the boundries between the granitoid

and country rocks are sharp and at the contact zone between metamorphics and the batholite intrusion, is characterized by 3 to 10 m's thick hornfels type rocks (Helvacı and Bozkurt, 1994). Enclaves of country rocks or previously crystallized granite occur in the batholite (Figure 2.4).

There are joints which formed probably during cooling of granitoid. Around those joints the granite had undergone pronounced alteration (Figure 2.5). Macroscopically granitoids of the region are grey and dark grey on fresh surfaces and yellow to red on altered surfaces. Granites are equigranular. Quartz, feldspar and amphibole minerals can be identified easily in hand specimens.

There are aplite and pegmatite dykes trending NE-SW and SE-NW. Their thicknesses range from 5 cm to 300-350 m. Especially around Oymaağaç region there are many aplite dykes cross-cutting each other. The dykes contain K-feldspar, quartz and small amounts of mafic minerals such as biotite and tourmaline. The boundry between the dykes and granitoid is sharp and straight (Figure 4.2). There are also pegmatite dykes other than aplite dykes which contain large quartz crystals, orthoclase and small amounts of tourmaline, beryl and rutile.

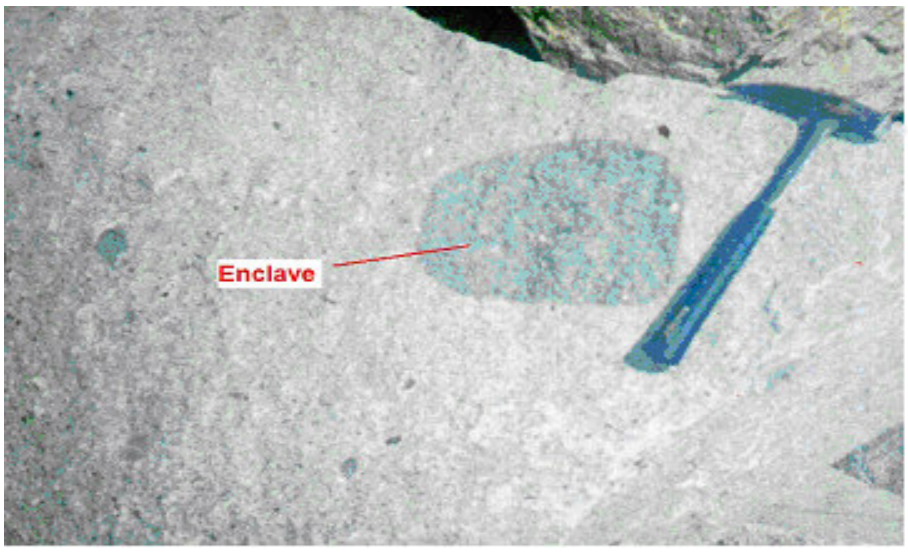

Figure 2.4. Enclave (3 km's away from Tacettin Village, old granite mine) (The handle of the geological hammer is 30 cm).

Figure 2.5. Highly altered granitoids around joints (2 km's away from Yassıkaya Köyü, near Kirmir Çayı).

The granitoid cuts the Palaeozoic metamorphics. Palaeocene, Eocene, and Miocene sediments overlie nonconformably these granitoids (Figure 2.6) (Helvacı and Bozkurt, 1994). The field relations suggest that the age of granitoid is bracketed between Permian and Palaeocene. Whereas if one consideres regional geology, a Late Cretaceous age can be envisaged.

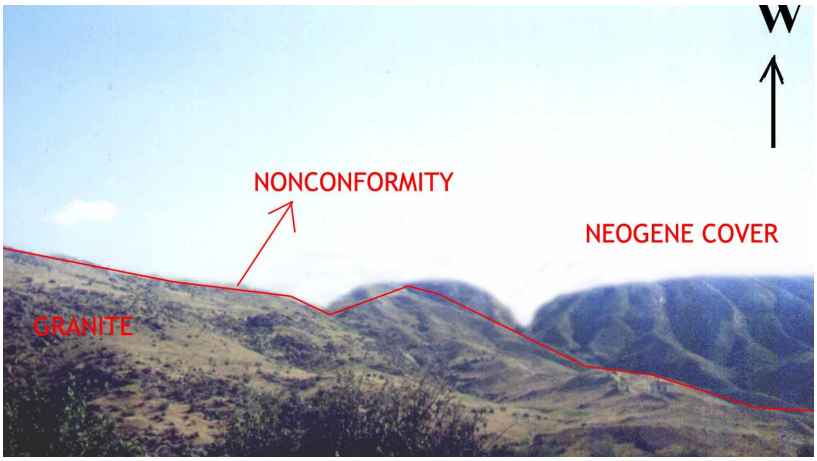

Figure 2.6. The non-conformity between sedimentary units and the granitoids (2 km's away from Yassıkaya Köyü, near Kirmir Çayı).

CHAPTER III

GEOLOGY

In this chapter, field observations are described. The region surrounding the study area includes three main units, (1) the Softa Formation (Kayakıran and Çelik, 1986) represented by gypsiferous mudstone and conglomerates, (2) the Tepeköy Metamorphics (Göncüoğlu *et al.*, 1992), and (3) Beypazarı Granitoid (Figure 3.1.). However, in this study area, no outcrop of Tepeköy Metamorphics are observed. In other words, the area is covered by sedimentary units and granites (Figure 3.2).

3.1. BEYPAZARI GRANITOID

The Beypazarı Granitoid is intruded into the metamorphics probably during Late Cretaceous (Helvacı and Bozkurt, 1991); continental Neogene sediments cover nonconformably the Beypazarı Granitoid (Figure 3.1).

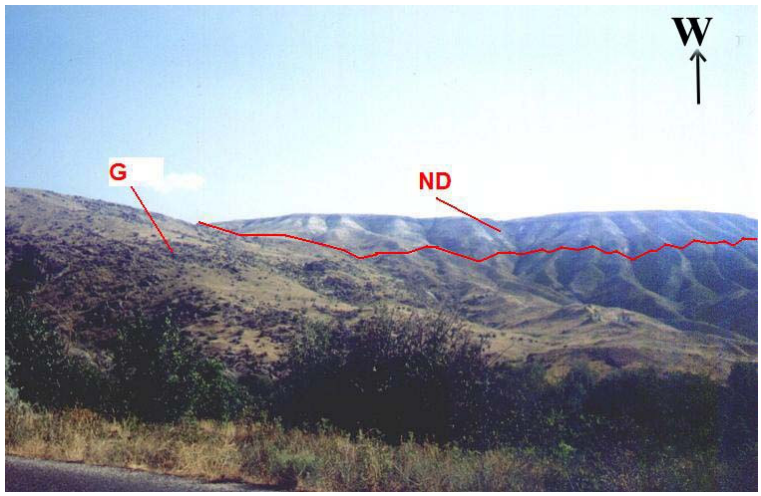

Figure 3.1. The view of the nonconformity; the granitoid (G) and the Neogene Deposits (ND). (4 km's away from Yassıkaya Köyü, near Kirmir Çayı)

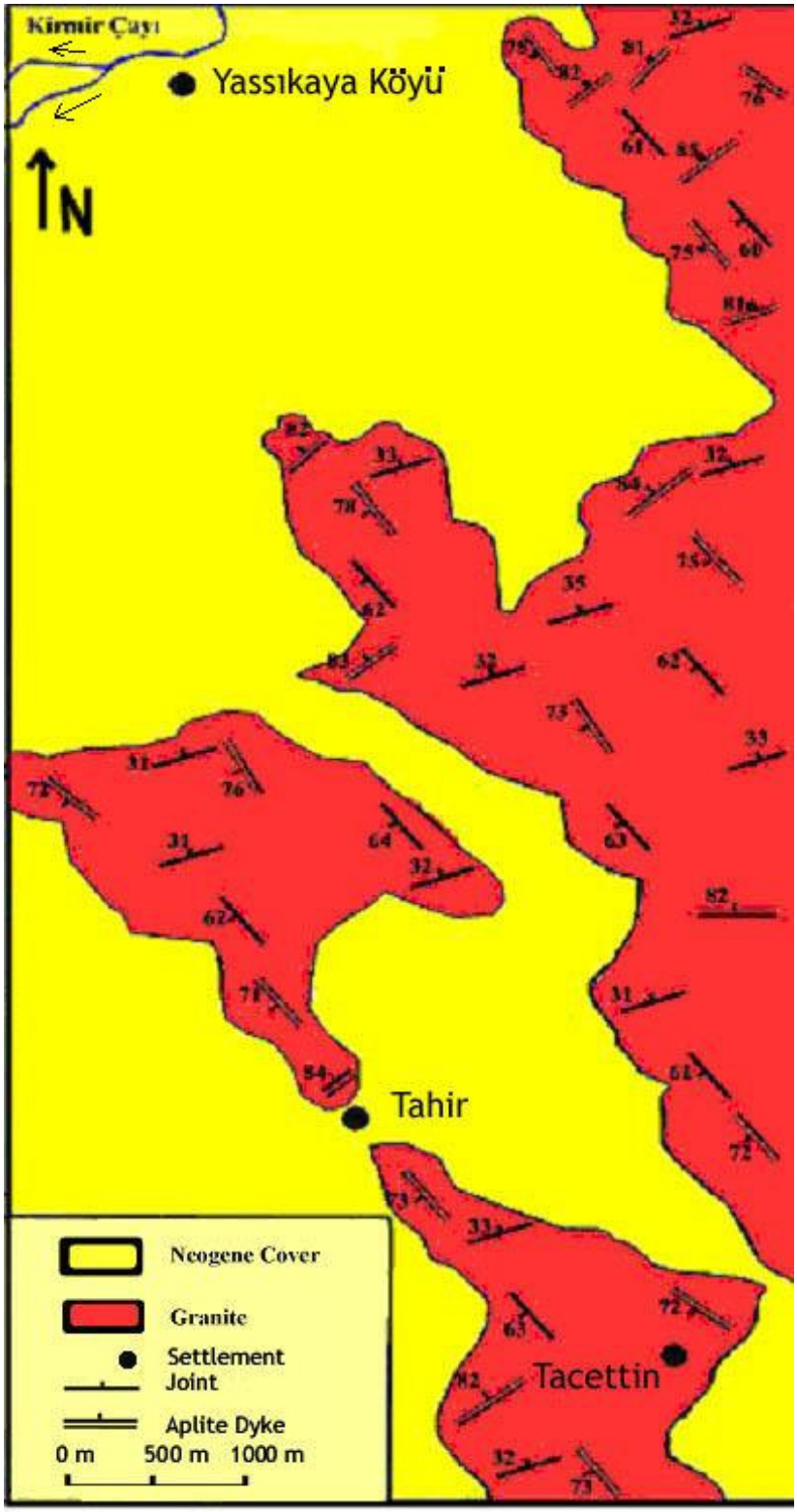

Figure 3.2. Geological map of the Yassıkaya Sector.

The granitoid contains enclaves (Figure 2.4). Aplite dykes and pegmatites are observed cutting the granitoid (Figure 3.3). Also a pegmatitic dyke is found cross-cutting the metamorphic complex (Yohannes, 1993). However, in the Yassıkaya region no pegmatitic dyke is observed.

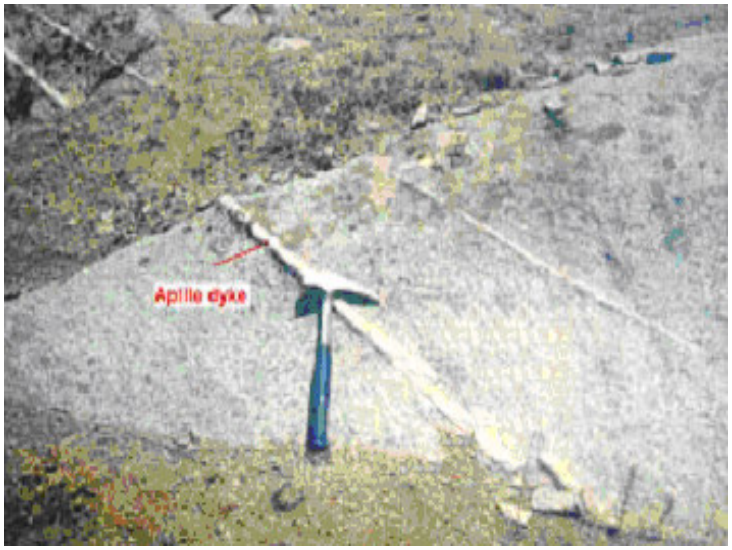

Figure 3.3. Aplite dyke cutting the granitoid (The handle of the geological hammer is 30 cm).

3.1.1. GRANITOID

The Beypazarı Granitoid displays a homogeneous composition around the study area. Petrographically (Chapter 4), with few exceptions, all samples display nearly the same composition; "quartz-rich granitoid". It is mainly composed of quartz (~40-75 %), K-feldspar (~5-15%), plagioclase (~15-30%), and hornblende (~3-15%).

The colour of K-feldspar is pink to pinkish grey around the region. Some K-feldspar grains are found as megacrysts of size ranging from a cm to 5-6 cm's (Figure 3.4). The size depends on the origin of K-feldspar, which may be either magmatic (phenocryst) or product of solid state replacement (porphyroblast).

Vernon (1986) has forwarded numerous characteristic features to identify phenocrysts from porphyroblasts (Yohannes, 1993). One of the features of Vernon is the alignment of K-feldspar megacryst within the matrix. Alignment of the long axis of megacryst suggests a rigid body rotation. In the field, a parallel alignment of K-feldspar megacrysts is observed therefore, the K-feldspar megacrysts are of magmatic origin.

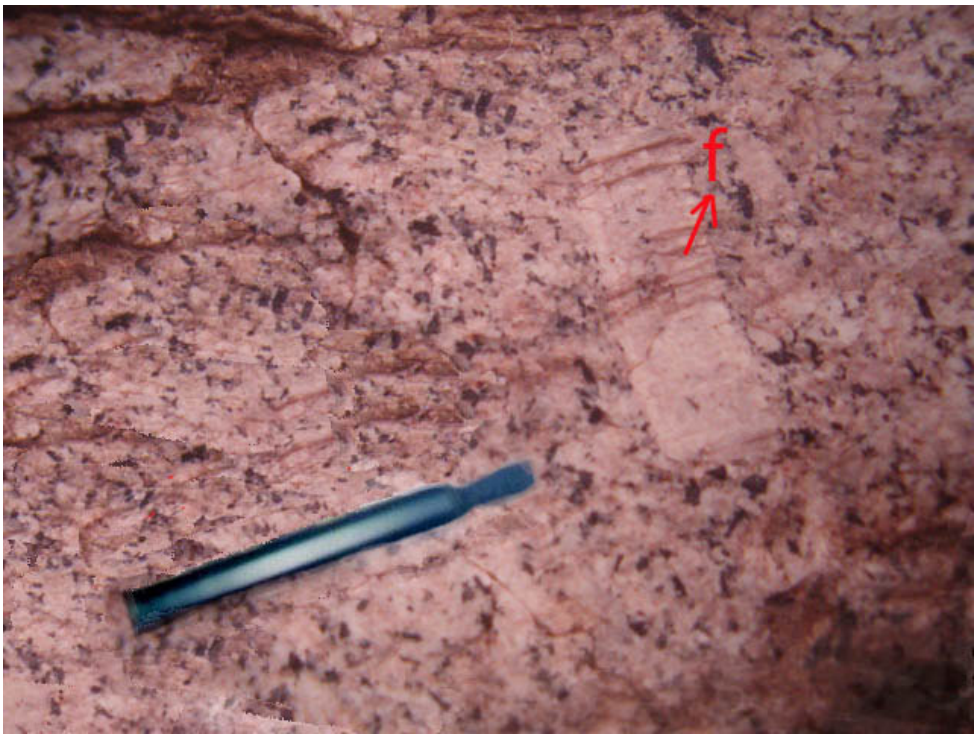

Figure 3.4. A close-up view of granitoid showing a K-Feldspar megacryst (f) (The pen is 14 cm long).

The large hornblende grains are subhedral to euhedral in handspecimens. The lineation of hornblende grains can not be seen since there were not enough large grains to be observed in hand specimens.

3.1.2. ENCLAVES

There are enclaves throughout the granite body, ranging from 1 cm to 1 m, spherical to ellipse shape, displaying elliptical cross-sections (Figure 3.5). Enclaves are mafic and fine-grained.

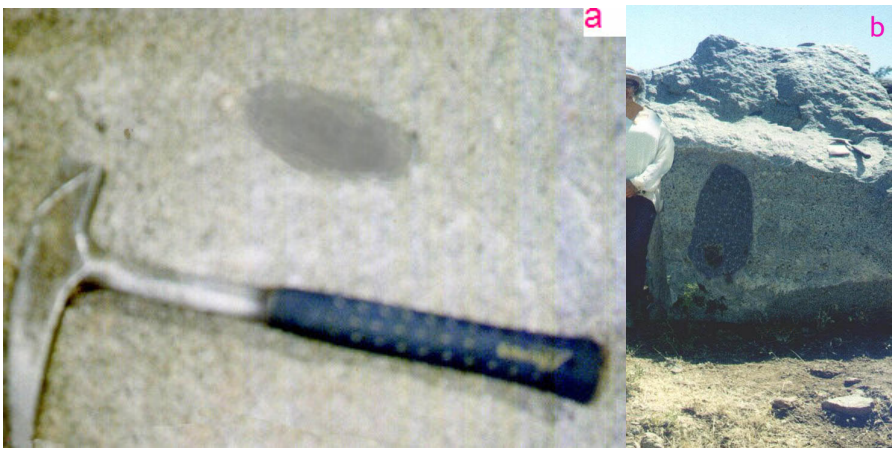

Figure 3.5. Elliptical cross-sections of enclaves observed, north of Tacettin Village ((a) The hammer is 30 cm, (b) The lady is 165 cm).

3.1.3. APLITE DYKES

There are various aplite dykes cross-cutting the granitoids throughout the study area in northeast-southwest and southeast-northwest direction. The aplite dykes are fine-grained compared to granitoids, and it has a dirty-sugary appearance. The boundry between aplite dyke and granitoid is sharp. (Figure 3.3).

3.2. SOFTA FORMATION

The "Softa Formation" name was given by Kayakıran and Çelik (1986). There are two rock units in the Softa Formation; gypsiferous mudstone and conglomerate. The Softa Formation overlies the metamorphics and the Beypazarı

Granitoid nonconformably (Figure 3.1); the age of this unit is therefore accepted to be Late Neogene (Kayakıran and Çelik, 1986).

3.2.1. GYPSIFEROUS MUDSTONE

This unit is characterized by alternating layers of mudstone and gypsum. The clay-rich layer is abundant around Dikmen and contains thin layers of siltstone (Yohannes, 1993). This unit exhibits variable thickness that ranges from a centimeter to tens of meters. The unit is completely devoid of fossils. However, according to P. de Tchihacheff in Kalafatçıoğlu and Uysallı (1964), this unit contains *Melanopsis costata*, a fossil of Late Neogene age.

3.2.2. CONGLOMERATE

The conglomerate has a uniform thickness of about one meter (Yohannes, 1993). It consists of large pebbles at its base and is represented by a fining upward sequence. The pebbles are granitic, metamorphic and mainly volcanic. The shape of pebbles are rounded to subrounded. The conglomerate is loosely cemented by gypsum.

3.3. ALLUVIUM

It is represented by sandy soil cover, which is used for agriculture and by blocks and boulders on the river bed . It covers large area; almost half of the study area is used for agriculture (Figure 3.6).

Figure 3.6. An agricultural field in the region (Area is near Kirmir Çayı, 1 km away from Yassıkaya Village).

3.4. STRUCTURE

The region is located on the collision belt between the Pontides and the Anatolides (Göncüoğlu *et al.* 2000). The metamorphic rock units are highly deformed. There are numerous folds, foliations, shear zones, faults and joints in the the region (Helvacı and Bozkurt, 1994). However, there are no folds, foliations, and shear zones in the study area except for the minor faults.

3.4.1. FAULTS

In this study area there is no megascopic fault. Only a minor fault exists cutting aplite dyke at Asar Tepesi (Figure 3.7).

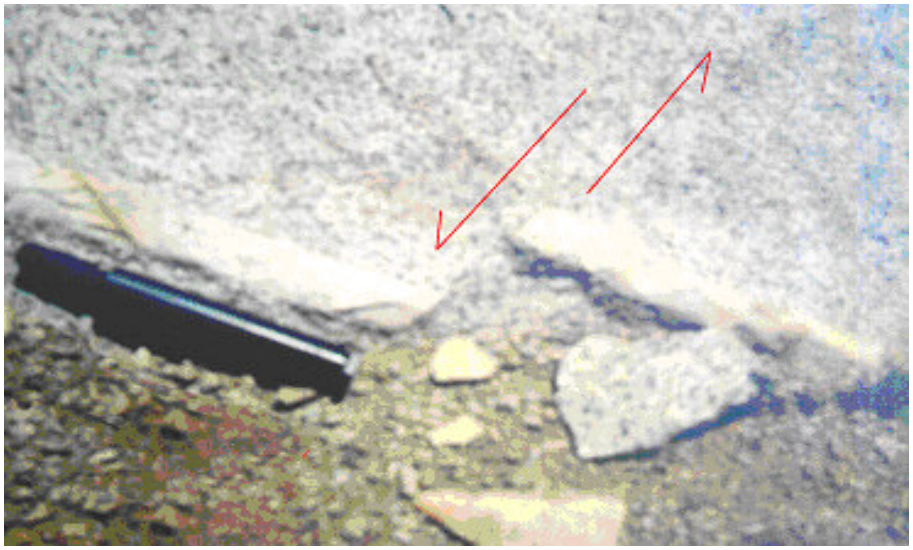

Figure 3.7. Minor fault cutting the aplite dyke (The pen is 14 cm long).

3.4.2. JOINTS

Joints in the region are oriented in NE-SW and NW-SE directions. A rose diagram from 20 measurements is prepared (Figure 3.8). This rose diagram clearly illustrates the presence of conjugate joint set indicating a principal stress aligned in NNW-SSE direction (Figure 3.8).

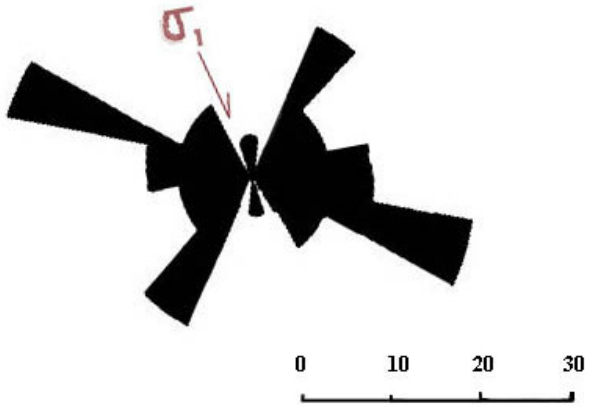

Figure 3.8. Rose Diagram of joints

According to Yohannes (1993), deformation is regional since the joints of metamorphic basement display the same direction with joints of granitoid. However, this stress alignment may be due to cooling of granitoid as suggested earlier.

CHAPTER IV

PETROGRAPHY OF BEYPAZARI GRANITOID

The field observations of Beypazarı Granitoid are described in the "geology" section (Chapter 3). In order to study the granitoid, petrography is utilized as one of the main tools. The results of petrographic investigations will be summarized in the following sections.

4.1. GRANITOID

From the study area, 36 relatively fresh samples were collected (Figure 4.1). In hand specimens, the granitoids are coarse grained, and in thin sections they display holocrystalline and hypidiomorphic textures. Before describing characteristic features of each mineral, the results of point counting analysis are outlined (Table 4.1). Between 1500 and 2500 points are counted for each sample to determine the percentages of the rock-forming minerals.

When the point-counting analysis for 36 samples are located on the QAP Streckeisen triangular diagram (Streckeisen, 1976), it is seen that samples match the "granite", "alkali-feldspar granite", and mainly the "quartz-rich granitoid" fields (Figure 4.2). The samples corresponding to the region "alkali-feldspar granite" represent aplite dykes. Except for a number of the samples most are classified as quartz-rich granitoid.

The granitoid is composed of quartz, alkali feldspar, plagioclase, pyroxene, hornblende, minor amounts of biotite, zircon, sphene, apatite, zeolite, and opaque minerals; calcite and sericite occur as alteration products. The characteristic features of each mineral are mentioned below.

Table 4.1. Modal analyses of rock forming minerals in the samples (volume %).

Minerals	Sample No					
	B1G1	**B1G2**	**B1G3**	**B1G4**	**B1G5**	**B1G6**
quartz	48,56	63,68	3,22	3,22	3,00	54,60
orthoclase	11,51	0,00	56,11	64,11	49,63	15,23
microcline	3,35	8,71	5,09	5,49	10,00	0,00
plagioclase	13,19	15,17	9,65	9,65	13,75	15,23
pyroxene	0,00	0,00	0,00	0,00	2,25	3,74
hornblende	6,48	5,47	16,00	8,00	4,63	3,45
biotite	11,65	2,99	6,18	6,18	4,00	2,01
zircon	0,24	0,49	0,00	0,00	0,00	0,00
sphene	0,00	0,00	0,00	0,00	0,00	0,00
apatite	3,10	0,00	3,35	3,35	2,75	0,00
opaque	1,92	3,48	0,00	0,00	5,10	5,75
zeolite	0,00	0,00	0,00	0,00	4,90	0,00

Minerals	Sample No					
	MG	**B1G4**	**B1G5**	**B2G2**	**B2G4**	**B2G5**
quartz	65,8	52,92	66,80	52,82	65,46	48,63
orthoclase	11,06	8,41	11,06	11,93	4,55	11,68
microcline	0,00	6,51	0,00	0,00	0,00	0,00
plagioclase	11,86	14,38	8,86	16,89	18,35	22,39
pyroxene	4,42	6,24	4,42	5,90	3,08	5,22
hornblende	3,54	4,21	3,54	4,02	3,24	4,26
biotite	0,00	0,81	0,00	0,00	2,93	0,00
zircon	0,00	0,00	0,00	0,00	0,00	0,00
sphene	0,00	0,81	0,00	0,00	0,00	0,00
apatite	2,36	0,81	2,36	3,62	0,00	4,95
opaque	0,95	4,07	2,95	4,83	3,39	2,88
zeolite	0,00	0,81	0,00	0,00	0,00	0,00

Table 4.1. Continued.

Minerals	Sample No					
	B2G6	**B3G2**	**B3G3**	**B3G5**	**B3A1**	**B3A2**
quartz	44,46	35,61	59,14	66,30	47,25	46,88
orthoclase	13,16	25,31	0,00	0,00	44,97	44,85
microcline	0,00	0,00	1,45	2,34	0,00	0,00
plagioclase	19,53	25,87	17,83	13,80	4,30	4,50
pyroxene	9,42	0,00	4,13	0,00	0,00	0,00
hornblende	5,26	3,34	8,39	5,73	1,74	1,89
biotite	0,00	5,15	0,00	0,00	0,94	0,00
zircon	0,00	0,00	0,00	0,00	0,00	0,00
sphene	0,00	0,28	0,00	0,00	0,00	0,00
apatite	3,32	0,00	4,39	3,24	0,94	0,00
opaque	4,85	4,45	4,66	8,59	3,22	1,89
zeolite	0,00	0,00	0,00	0,00	0,00	0,00

Minerals	Sample No					
	B3A3	**B3A4**	**B3A5**	**B4G1**	**B4G3**	**B4G4**
quartz	44,19	45,67	47,42	62,73	41,82	45,37
orthoclase	41,18	41,56	43,01	7,24	0,00	10,02
microcline	0,00	0,00	0,00	2,49	11,35	3,97
plagioclase	7,17	4,70	4,86	13,27	25,46	24,39
pyroxene	0,00	0,00	0,00	4,69	0,00	0,00
hornblende	0,00	0,00	0,00	13,49	14,51	6,05
biotite	0,00	3,08	0,00	3,09	5,15	5,48
zircon	0,00	0,00	0,00	0,00	0,00	0,00
sphene	0,00	0,00	0,00	0,00	0,00	0,00
apatite	4,88	2,94	2,58	0,00	0,00	0,00
opaque	2,58	2,06	2,13	2,98	1,72	4,73
zeolite	0,00	0,00	0,00	0,00	0,00	0,00

Table 4.1. Continued.

Minerals	Sample No					
	B4G6	**B5G1**	**B5G2**	**B5G3**	**B5G4**	**B5G5**
quartz	23,96	30,40	49,08	4,37	66,10	54,64
orthoclase	0,00	0,00	0,00	58,83	8,71	0,00
microcline	16,94	9,94	7,37	12,39	1,07	7,00
plagioclase	40,90	22,16	25,80	13,02	9,79	13,24
pyroxene	0,00	0,00	1,51	0,00	0,00	0,00
hornblende	12,97	15,06	13,40	5,12	9,80	14,31
biotite	3,24	0,00	0,00	3,02	0,00	0,00
zircon	0,00	0,00	0,00	0,00	0,00	0,00
sphene	0,00	0,43	0,00	0,55	0,36	0,00
apatite	0,00	17,47	0,00	0,00	2,36	5,02
opaque	1,98	4,55	2,85	2,19	1,81	5,78
zeolite	0,00	0,00	0,00	0,52	0,00	0,00

Minerals	Sample No					
	B5G6	**B5A1**	**B5A2**	**B6G2**	**B6G4**	**B6G6**
quartz	49,13	44,82	47,04	54,53	56,53	39,13
orthoclase	11,30	45,66	41,40	9,06	14,06	11,54
microcline	0,00	0,00	0,00	0,00	0,00	0,00
plagioclase	20,72	3,78	4,81	12,03	9,03	15,55
pyroxene	0,00	0,00	0,00	0,00	4,00	0,00
hornblende	13,04	0,00	4,40	8,40	8,40	18,73
biotite	0,00	0,00	0,00	10,71	5,71	9,36
zircon	0,00	0,00	0,00	0,00	0,00	0,00
sphene	0,00	0,00	0,41	0,00	0,00	0,00
apatite	2,17	2,66	0,00	0,00	0,00	0,00
opaque	3,62	3,08	1,93	5,27	1,27	3,51
zeolite	0,00	0,00	0,00	0,00	0,00	2,17

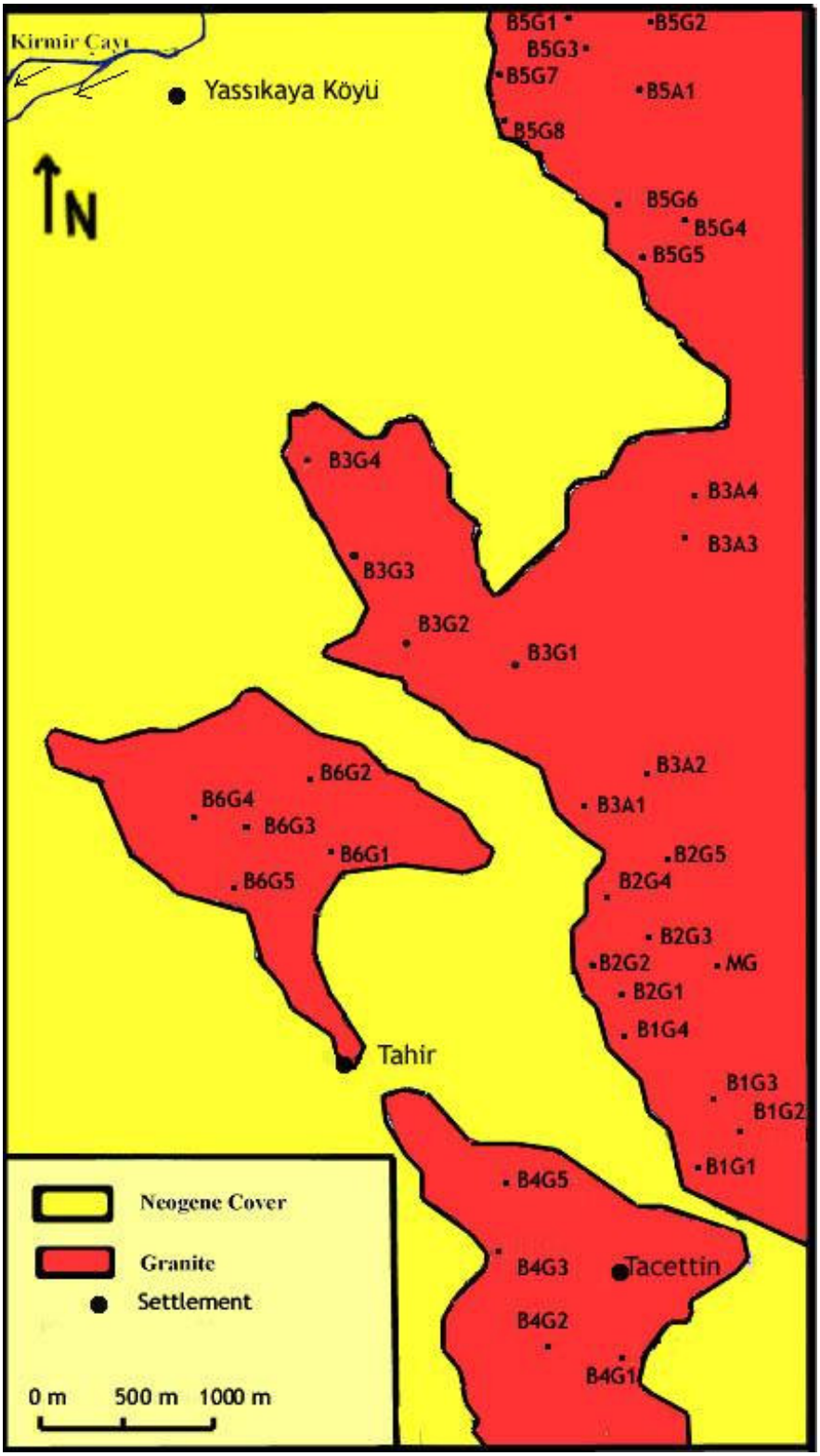

Figure 4.1. The sample location map of the Beypazarı Granitoid, Yassıkaya Sector.

Quartz: Quartz is the major component of the granite. It has an anhedral crystal outline. Quartz grains are coarse, but finer than the plagioclase and the alkali feldspar grains. In the study area, euhedral quartz crystals are not common. In some granitoids, quartz displays graphic texture (Figure 4.3), where wormlike, irregular but optically continuous grains of quartz are intergrown with feldspar. According to Raymond (2001), this texture is favored by rapid rates of cooling, large degrees of undercooling, and fewer heterogeneous nucleation sites.

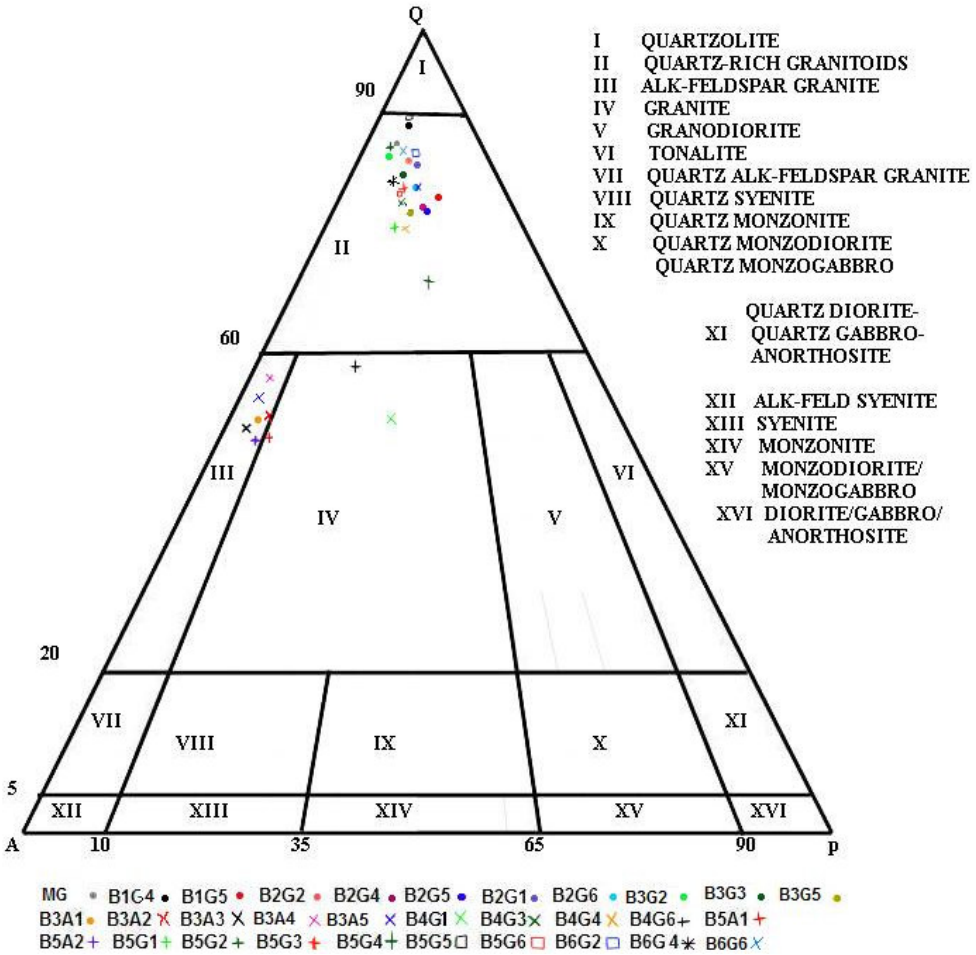

Figure 4.2. Plot of samples on the Streckeisen (1976) triangular QAP diagram.

Alkali Feldspar: Common to many plutonic rocks (Raymond, 2001) the study area granitoid contains K-feldspar that display anhedral to subhedral crystal outline. Orthoclase and microcline are common K-feldspars in the studied samples. Orthoclase occurs as subhedral and anhedral crystals (Figure 4.4) and shows Carsbald twinning with simple twins consisting of two individuals.

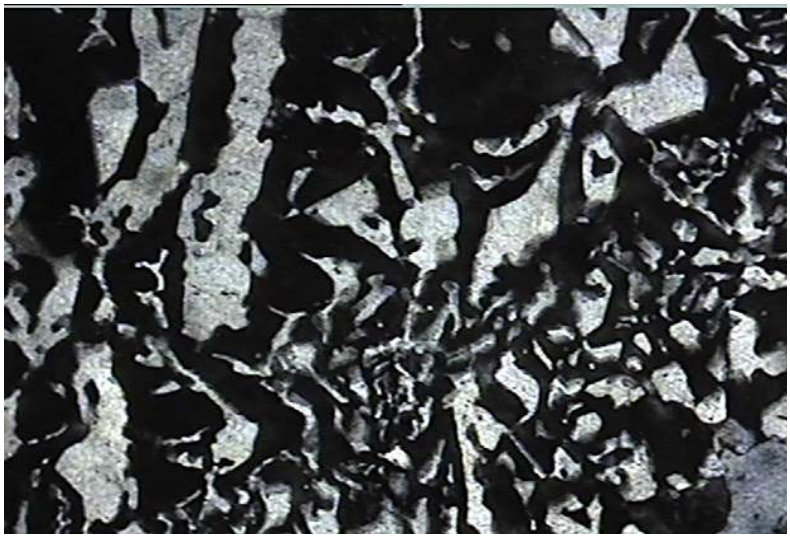

Figure 4.3. Graphic texture displayed by quartz and orthoclase (Sample B1G3, 4X, XPL).

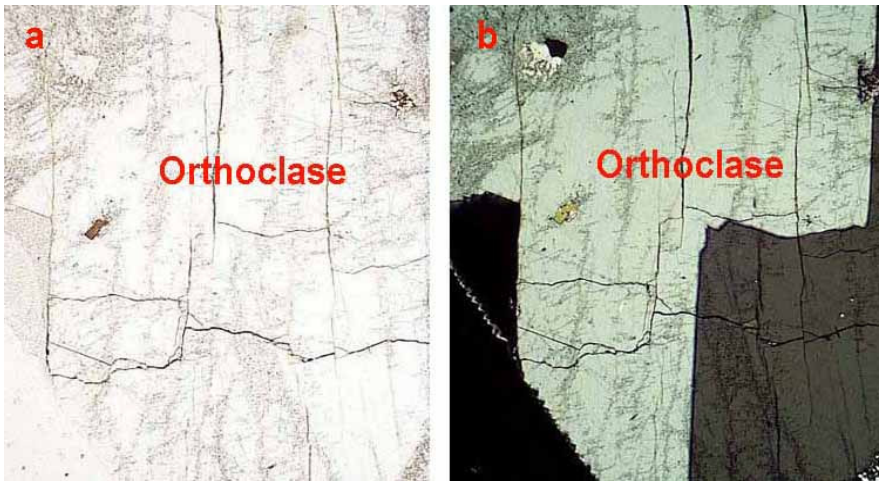

Figure 4.4. Orthoclase crystal (Sample B1G1, 40X, (a) PPL, (b) XPL).

Microcline also occurs as subhedral to anhedral crystals. It displays polysynthetic twinning where the twinning is in two directions, one obeys albite law ([010]=twin plane), and the other, pericline law (b axis or [010]=twin axis) (Figure 4.8). This texture is known as quadrille structure, characterized by the two sets of twin lamellae which are at right angles (Kerr, 1959).

Plagioclase: Plagioclase is defined by its characteristic polysynthetic twinning (Figure 4.5). The grains have subhedral crystal outline. The type of plagioclase is determined by the Michel-Lévy Method where, at least, eight different crystals were measured to find out the maximum extinction angle of a particular plagioclase. The results are consistent with an "andesine" composition for plagioclases of studied samples.

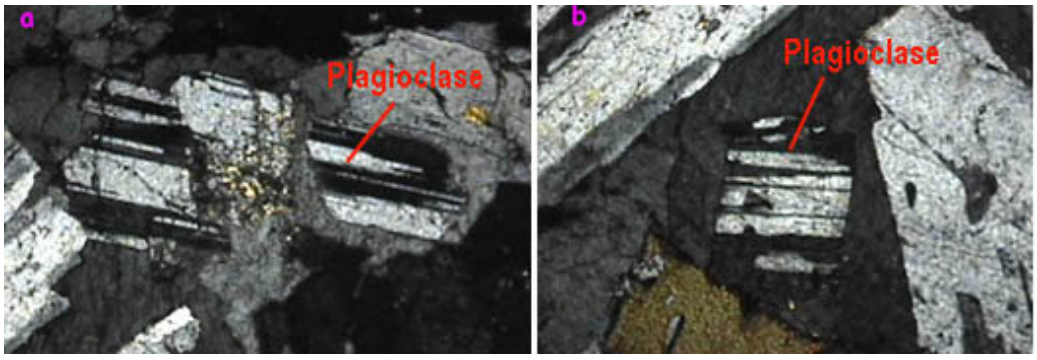

Figure 4.5. Plagioclase ((a) Sample B2G3, 4X, XPL, (b) Sample B2G2, 4X, XPL).

Pyroxene: Pyroxene is euhedral, sometimes with octagonal crystal sections, with two cleavage sets oriented perpendicular to each other (Figure 4.6).

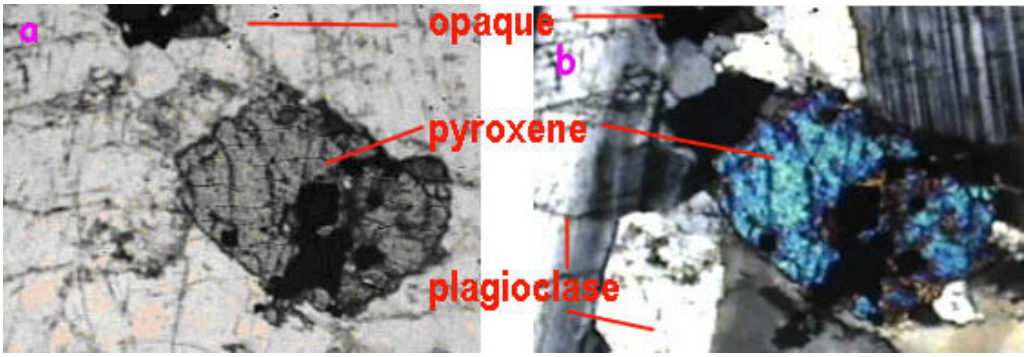

Figure 4.6. Pyroxene crystal (Sample B3G2, 4X, (a) PPL (b) XPL).

Hornblende: Hornblende crystals are subhedral to euhedral and displays sometimes hexagonal-shape, and are pleochroic from bluish green to brownish green. The two sets of cleavage cutting each other in 56 degrees are clearly seen in many of the rhombic sections (Figure 4.7). In some samples, chloritization is common. Large grain size, subhedral to euhedral crystal shape indicate that, hornblende began to crystallize early, and continued for an extended time.

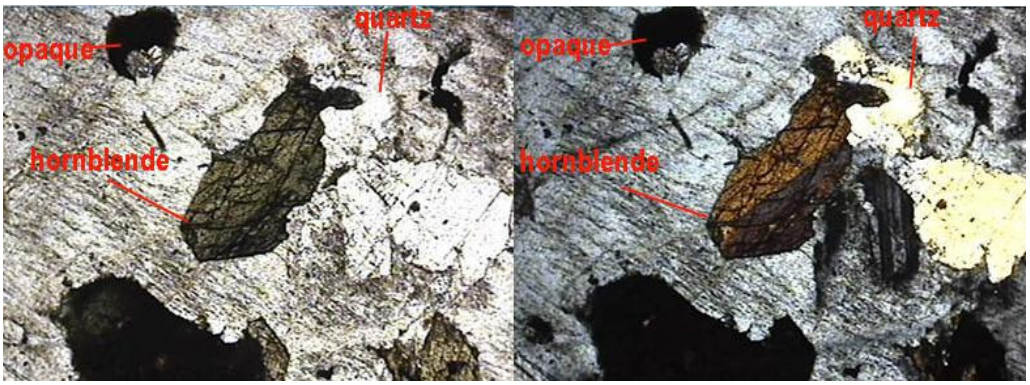

Figure 4.7. Subhedral hornblende crystal, displaying rhombus (diamond)-shape, and the two sets of cleavage (56˚) (Sample B1G2, 4X, XPL and PPL views).

Biotite: Biotite occurs as subhedral crystals. It has brown pleochroism and displays short tabular outline. In most samples, poikilitic texture is characteristic with

opaque minerals as inclusions (Figure 4.8). Chloritization is common alteration type seen in biotites.

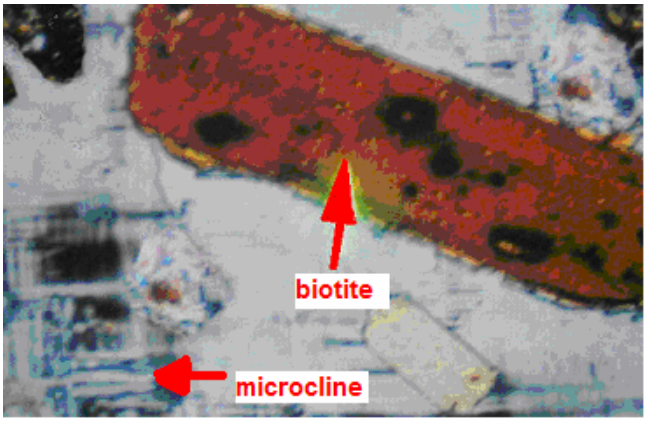

Figure 4.8. Subhedral biotite crystal, showing brown pleochroism (Sample B1G1, 4X, XPL).

Opaque Minerals: Since most of the opaque minerals are black, they can be hematite, ilmenite or magnetite (Figure 4.9).

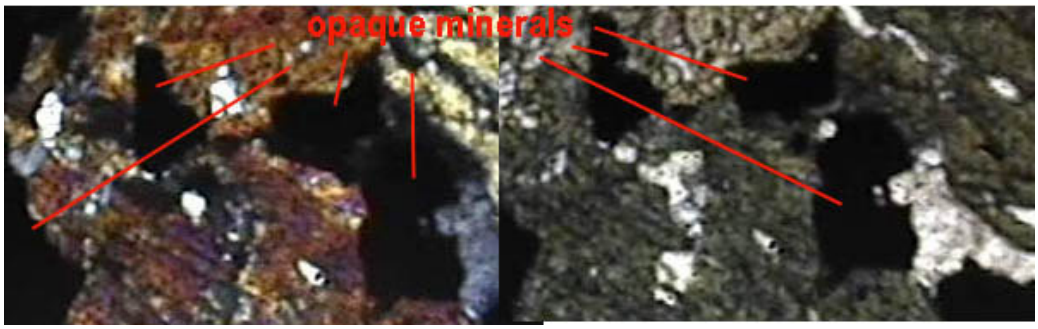

Figure 4.9. Opaque minerals (Sample B3G4, 4X, (a) XPL, (b) PPL).

Sphene: Sphene is found as euhedral, wedge-shaped crystal with high relief (Figure 4.10). It is not a common accessory mineral. Its well developed, euhedral

shape is an indicator of an early phase crystallization. In sample B5G3, sphene displays simple twinning (Figure 4.10).

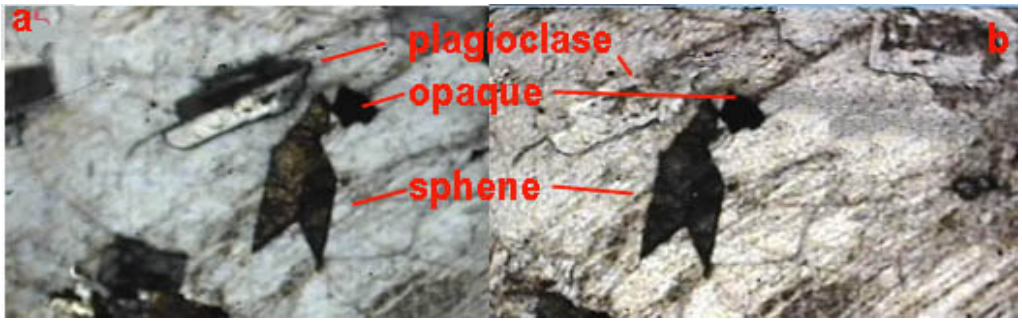

Figure 4.10. Euhedral, wedge-shaped sphene crystals showing twinning (Sample B5G3, 4X, (a) XPL, (b) PPL).

Apatite: Apatite is a common accessory mineral which occurs as inclusions in plagioclases or as well-developed, euhedral, hexagonal individual crystal outline (Figure 4.11). It has black-grey interference colour. They display no cleavage, and moderate relief.

Zircon: It occurs commonly as inclusions in plagioclases. The crystals have well-developed, euhedral section with no cleavage; and display very high relief (Figure 4.11). It is distinguished from apatite by stronger birefringence and higher relief.

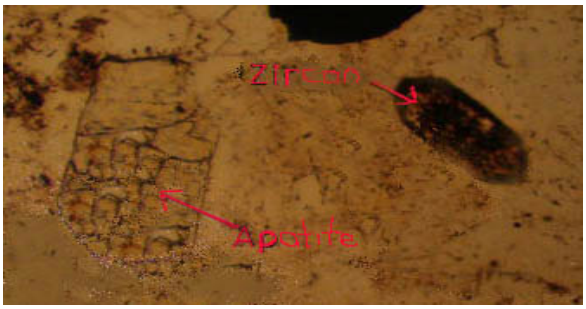

Figure 4.11. Well-developed, euhedral, hexagonal apatite crystal and well-developed, euhedral zircon with no cleavage and very high relief (Sample B1G1, 60X, PPL).

Zeolite: It is not a common mineral throughout the granite body. Zeolite has black-grey interfence colour like apatite. It is distinguished from apatite by the presence of cleavage and its low refractive index than canada balsam. It fills the empty spaces between the grains.

Chlorite: Chlorite is usually found as alteration product of hornblende or biotite. It has typical green pleochroism and define a radial pattern with very low birefringence.

Sericite: Sericite is hydrothermal alteration product of feldspars. It is not commonly found in the thin sections of the granite body.

4.2. ENCLAVES

The enclaves are found with elliptical sections and very sharp contact relationship with the host granitoid. The mineralogical content of enclaves is dioritic; in other words, hornblende, plagioclase, and pyroxene occur as common minerals, whereas sphene and chlorite, minor minerals. The dominant mineral, pyroxenes occur as large octagonal crystal outlines. Chlorites occur as late stage alteration products.

4.3. APLITE DYKES

The aplite dykes mainly contain K-feldspar, quartz, hornblende, biotite, opaque minerals, and rarely apatite. Alteration is not common in sections. On the contrary the minerals are well-developed, and very fresh. Quartz grains are finer than those in granitoid. In some samples, graphic texture is observed (Figure 4.3). Quartz crystals are grown interlocked with K-feldspar crystals in a way resembling cuneiform, that's why this texture is called graphic texture.

CHAPTER V

PETROCHEMISTRY

In addition to field observation and petrographic study, petrochemistry is also a necessary tool to study the granitoids. Their tectonic environment, origin, and processes involved during their ascent can be determined by their chemical composition which is an important key reflecting the history of granitoids starting from source to the end of their evolution. Each rock has its own major and trace element compositions, in other words, major and trace element compositions obtained as a result of chemical analysis are finger-prints helping to outline the overall history of granitoids in conjunction with field and petrographic observation.

Granitoids are classified either by their mineralogical and chemical characteristics or by their tectonic settings and geologic occurence. There are mainly four types of granitoids according to their mineralogical and chemical characteristics; I-type, S-type (Chappel and White, 1974), M-type and A-type (Collins *et al.* 1982). According to tectonic setting and geologic occurence, granitoids are classified as Ocean-Ridge Granitoids (ORG), Volcanic-Arc Granitoids (VAG), Within Plate Granitoids (WPG), and Collision Granites (COLG) according to Pearce *et al*. (1984) using trace element data. Whereas, using major oxide data, Maniar and Piccoli (1989) classified granitoids as island-arc granitoids (IAG), continental-arc granitods (CAG), continental-collision granitoids (CCG), post-orogenic granitoids (POG), continental epeirogenic uplift granitoids (CEUG), rift-related granitoids (RRG), and oceanic plagiogranite (OP), where ORG corresponds to OP, VAG corresponds to IAG and CAG, and COLG corresponds to CCG.

Several diagrams are used to interpret the petrochemical data. Many techniques are developed to identify the tectonic settings, origins, and cooling histories of granites. The Shand's index (Shand, 1951), is used for its geochemical discrimination. The subdivisions are peraluminous, metaluminous, and peralkaline

according to the alumina and alkali content (Maniar and Piccoli, 1989), assuming the metaluminous granites are products of volcanic-arc granitoids, alkaline and peralkaline magmas are related to the within plate tectonic setting and peralumious granites are the result of partial melting of the continental crust. White and Chappel (1977) subdivided the granites into I- and S-types giving idea about their tectonic setting. Origin of S-type granites are assumed to be continental collision and origin of I-type granites are assumed to be the result of continental arc and post-orogenic magmatism (Pearce *et al.* 1984). Related to above assumptions, other classifications are made by Collins *et al.* (1982): A-type granitoids belonging to anorogenic tectonic setting and by White (1979): M-type granitoids resulting from island arc magmatism. All these classifications are inconvinient to use alone since they do not have well-defined boundries between tectonic settings. As a result, several discrimination diagram were prepared. The major element discrimination diagrams (Maniar and Piccoli, 1989) and trace element discrimination diagrams (Pearce *et al.*, 1984) subdivided the granites into tectonic settings with well defined boundries.

12 samples from the study area were analysed for major oxide (Table 5.1), trace element (Table 5.2) and REE compositions (Table 5.3).

Table 5.1. Major Oxide Compositions (wt %)

Sample	**B5G4**	**B6G6**	**B6G4**	**B4G1**	**B4G3**	**B3G3**	**B3G5**	**B2G4**	**B1G5**	**B1G4**	**B1G2**	**MG**
SiO_2	66,05	62,37	56,70	62,71	62,10	59,45	66,59	65,30	66,48	64,60	66,75	65,00
Al_2O_3	15,27	15,71	17,55	15,37	16,01	13,97	15,44	14,99	15,61	15,44	15,19	15,23
Fe_2O_3	4,39	5,81	6,69	6,25	6,08	4,16	3,94	4,84	3,79	4,30	3,99	4,73
MgO	0,92	2,23	2,97	2,25	2,30	1,32	1,05	1,61	1,17	1,27	1,33	1,57
CaO	3,84	5,27	7,48	5,12	5,42	4,25	3,92	4,77	3,87	4,84	4,00	4,51
Na_2O	3,30	2,85	3,33	1,77	2,81	2,83	3,01	3,02	2,99	3,15	2,98	3,13
K_2O	4,16	3,43	1,98	3,49	3,34	4,17	4,48	3,91	4,47	4,36	4,29	4,73
TiO_2	0,45	0,52	0,65	0,54	0,57	0,41	0,38	0,43	0,40	0,41	0,41	0,40
P_2O_5	0,17	0,17	0,18	0,18	0,16	0,16	0,14	0,17	0,15	0,16	0,15	0,15
MnO	0,06	0,13	0,15	0,13	0,13	0,10	0,07	0,12	0,08	0,11	0,09	0,12
Cr_2O_3	0,067	0,048	0,046	0,045	0,047	0,046	0,078	0,050	0,050	0,038	0,049	0,067
LOI	1,20	1,30	2,10	1,00	0,90	9,00	0,80	0,70	0,80	1,20	0,70	0,20
SUM	99,88	99,85	99,84	99,86	99,88	99,86	99,90	99,91	99,86	99,88	99,92	99,85

Table 5.2. Trace Element compositions (ppm)

Sample	B5G4	B6G6	B6G4	B4G1	B4G3	B3G3	B3G5	B2G4	B1G5	B1G4	B1G2	MG
Be	2,0	1,0	<1	2,0	1,0	<1	<1	2,0	3,0	2,0	2,0	<1
Co	7,5	10,9	14,2	12,4	13,1	8,5	10,4	9,8	7,9	8,7	8,9	11,0
Cs	2,3	3,1	2,0	3,0	2,9	2,8	3,1	2,7	3,3	2,7	3,0	3,3
Ga	17,1	17,4	19,2	17,6	16,6	16,8	17,7	16,5	15,3	15,6	17,2	17,8
Hf	4,0	3,9	3,8	4,1	3,9	3,8	3,5	4,0	3,4	3,3	3,6	3,9
Nb	13,3	10,7	9,7	10,6	10,6	11,8	10,0	11,2	10,2	10,3	10,6	10,4
Rb	165,3	100,4	47,7	111,9	102,0	187,2	206,7	184,3	176,2	171,0	182,9	202,2
Sn	2	2	2	2	2	1	1	2	2	1	2	2,0
Sr	547,5	473,7	602,1	428,3	441,2	505,5	539,6	472,7	489,3	520,9	484,4	516,1
Ta	0,9	0,8	0,6	0,8	0,9	0,8	0,6	0,7	0,7	0,7	0,7	0,6
Th	13,8	13,0	6,7	16,4	10,8	16,6	23,5	25,5	27,4	26,2	26,7	15,5
U	2,1	2,7	1,5	4,1	2,7	5,7	2,2	7,1	3,4	9,1	3,4	6,3
V	116	120	164	122	112	89	86	101	82	92	94	98,0
W	2,3	0,7	1,6	0,8	0,4	0,5	1,2	0,4	1,5	1,0	1,1	0,4
Zr	124,3	125,2	126,0	129,8	128,7	122,6	108,8	126,2	110,1	112,1	120,7	119,6
Y	23,5	26,6	23,0	22,1	23,1	23,4	17,6	19,7	18,8	17,7	19,2	18,4
Mo	11,9	8,4	8,5	7,3	8,4	8,9	15,9	9,1	10,0	7,4	9,3	33,6
Cu	18,4	16,1	19,2	20,8	16,7	14,6	33,7	14,1	20,5	12,2	19,3	51,6
Pb	3,4	7,4	7,0	4,7	6,2	5,9	2,3	4,9	2,8	5,3	2,5	5,2
Zn	27	35	52	37	39	20	16	21	17	18	16	19,4
Ni	27,7	23,0	20,3	15,6	17,9	23,1	32,5	20,7	23,0	16,8	20,2	21,5
As	6,3	0,9	1,1	1,0	0,7	1,0	1,8	1,1	3,7	1,2	2,9	1,1
Cd	<0,1	<0,1	<0,1	<0,1	<0,1	<0,1	<0,1	<0,1	<0,1	<0,1	<0,1	<0,1
Sb	0,4	0,1	0,2	<0,1	0,1	0,1	0,1	0,1	0,1	0,1	0,1	0,1
Bi	0,1	0,1	0,1	<0,1	0,1	0,1	<0,1	<0,1	0,1	0,1	0,1	<0,1
Ag	<0,1	<0,1	<0,1	<0,1	0,1	<0,1	<0,1	<0,1	<0,1	<0,1	<0,1	0,1
Au	0,5	<0,5	<0,5	<0,5	0,8	<0,5	0,5	<0,5	<0,5	<0,5	<0,5	1,4
Hg	<0,01	0,01	<0,01	<0,01	0,01	0,01	<0,01	<0,01	<0,01	<0,01	<0,01	0,0
Tl	<0,1	0,1	<0,1	0,2	0,2	<0,1	<0,1	<0,1	<0,1	<0,1	<0,1	<0,1
Se	<0,5	<0,5	<0,5	<0,5	<0,5	<0,5	<0,5	<0,5	<0,5	<0,5	<0,5	<0,5

5.1. ANALYTICAL METHODS

Before analysis, samples are prepared with painstaking processes because, contamination between samples causes wrong analysis results . The freshest part of each sample is separated carefully, and crushed into pieces of one or two centimeters by “jaw crusher”. Following this, process those centimetric pieces are powdered by another crusher. After each process, both machines are cleaned carefuly with air compressor in order to prevent contamination of samples with powder of each other.

Chemical analysis of prepared sample powders is made in ACME Analytical Laboratories.

Table 5.3. Rare Earth Element compositions (ppm)

Sample	**B5G4**	**B6G6**	**B6G4**	**B4G1**	**B4G3**	**B3G3**	**B3G5**	**B2G4**	**B1G5**	**B1G4**	**B1G2**	**MG**
La	39,7	35,5	24,9	22,7	25,6	36,8	35,1	37,1	32,7	34	34,9	33,6
Ce	71,8	67,7	50,2	44,6	48,9	57,8	52,1	58,7	53,7	56,6	57,2	51,6
Pr	7,06	7,25	5,96	5,17	5,97	6,53	5,36	5,8	5,55	5,59	6	5,17
Nd	27,1	30	26,2	21	25,1	24,8	22,4	23,2	20,8	20,2	21,9	19,4
Sm	4,5	5,3	4,5	4,2	4,2	4,3	3,7	3,9	3,5	3,9	3,9	3,7
Eu	1,12	1,2	1,26	1,01	1,21	1,09	0,9	1	0,95	1,03	0,96	1
Gd	4,19	4,49	4,82	4,02	4,46	4,3	3,46	3,57	3,36	3,38	4,08	3,1
Tb	0,7	0,85	0,68	0,56	0,66	0,58	0,47	0,59	0,52	0,51	0,58	0,4
Dy	3,62	4,57	4,02	2,76	3,73	3,77	2,95	3,12	2,96	3,12	3,15	2,8
Ho	0,81	0,84	0,76	0,72	0,75	0,75	0,53	0,67	0,63	0,64	0,63	0,6
Er	2,29	2,71	2,3	2,18	2,25	2,17	1,76	2,1	1,97	1,84	1,91	1,8
Tm	0,36	0,4	0,34	0,36	0,38	0,33	0,27	0,35	0,33	0,31	0,32	0,3
Yb	2,48	2,59	2,26	2,44	2,43	2,3	2,06	2,16	1,94	2,16	2,5	2,2
Lu	0,39	0,35	0,34	0,36	0,33	0,34	0,31	0,31	0,34	0,33	0,35	0,3

5.2. ROCK CLASSIFICATION

Before tectonic discrimination, rock classification should be made. For this purpose, several rock classification diagrams are used. According to Na_2O+K_2O vs SiO_2 diagram of Peacock, (1931) (Figure 5.1) the samples are of calcic and calc-alkalic origin.

Although, the following diagrams are used for rocks of volcanic origin, the result can be converted to plutonic rock type of same composition. According to Na_2O+K_2O vs SiO_2 diagram of Cox *et al*. (1979) (Figure 5.2), the samples fall in the dacite, andesite, trachyandesite regions. But, using SiO_2 vs Zr/TiO_2 (Figure 5.3) and Zr/TiO_2*0.0001 vs Nb/Y (Figure 5.4) diagrams of Winchester and Floyd (1977) is more accurate then Na_2O+K_2O vs SiO_2 diagram of Cox *et al*. (1979) since Zr and Ti are not mobile elements. According to SiO_2 vs Zr/TiO_2 diagram of Winchester and Floyd (1977) (Figure 5.3), the samples fall in the rhyodacite-dacite and andesite regions. Whereas Zr/TiO_2*0.0001 vs Nb/Y diagram indicates that these samples fall

in the area of rhyodacite-dacite and andesite regions (Winchester and Floyd, 1977). Therefore, the equivalent plutonic samples are granite, granodiorite, and diorite in compostion.

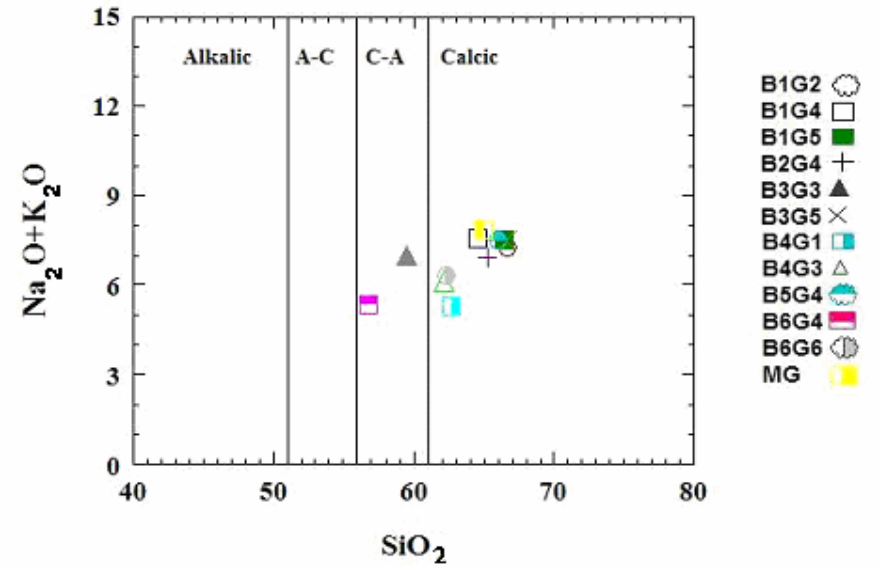

Figure 5.1. Na_2O+K_2O vs SiO_2 diagram (Peacock, 1931); A-C: alkali-calcic, C-A: calc-alkalic.

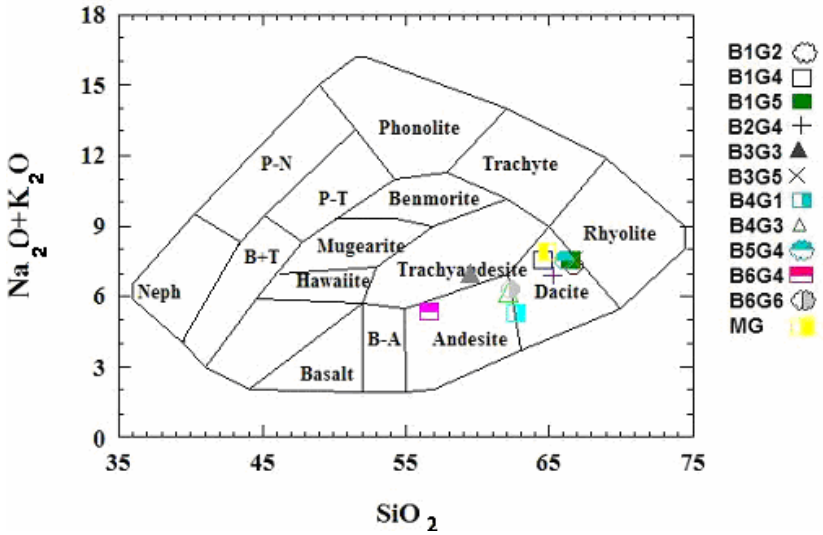

Figure 5.2. Na_2O+K_2O vs SiO_2 diagram (Cox *et al.* 1979); B-A: basaltic andesite, B-T: basaltic trachyte,Neph: nephelinite, P-N: phonolitic nephelinite, P-T: phonolitic trachyte.

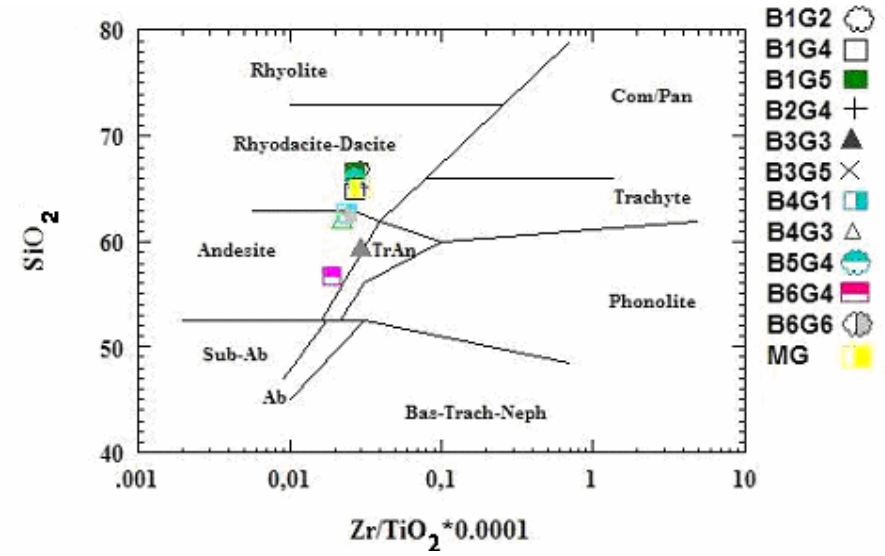

Figure 5.3. SiO_2 vs Zr/TiO_2 diagram (Winchester and Floyd, 1977); Ab: andesite-basalt, Bas: basanite, Com: comendite, Neph: nephelinite, Pan: pantellerite, Sub-Ab: sub-alkaline basalt, Trach: trachyte, Tr-An:trachy andesite.

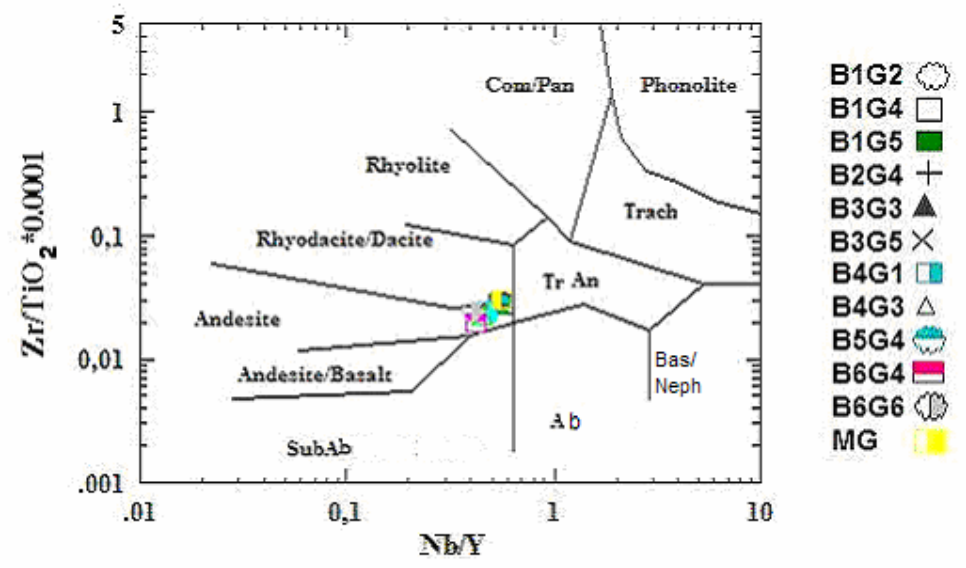

Figure 5.4. Zr/TiO_2*0.0001 vs Nb/Y diagram (Winchester and Floyd, 1977) ; Ab: andesite-basalt, Bas: basanite, Com: comendite, Neph: nephelinite, Pan: pantellerite, Sub-Ab: sub-alkaline basalt, Trach: trachyte, Tr-An:trachy andesite.

5.3. MAGMATIC EVOLUTION

Major oxide and trace element data helps to understand the crystallization history of Beypazarı Granitoids. In section 5.4 fractional crystallization, magma mixing and assimilation will be mentioned.

5.3.1. FRACTIONATION PROCESS

SiO_2 content is the mostly used, index oxide in Harker Diagrams (Harker, 1909). The negative slope in distribution of samples on Fe_2O_3 vs SiO_2 (Figure 5.5), CaO vs SiO_2 (Figure 5.6), MgO vs SiO_2 (Figure 5.7), Al_2O_3 vs SiO_2 (Figure 5.8), MnO vs SiO_2 (Figure 5.11), TiO_2 vs SiO_2 (Figure 5.12) and P_2O_5 vs SiO_2 (Figure 5.13) diagrams corresponds to fractional crystallization. In K_2O_3 vs SiO_2 diagram (Figure 5.9), samples display a positive trend therefore K_2O is also reflecting fractionation.

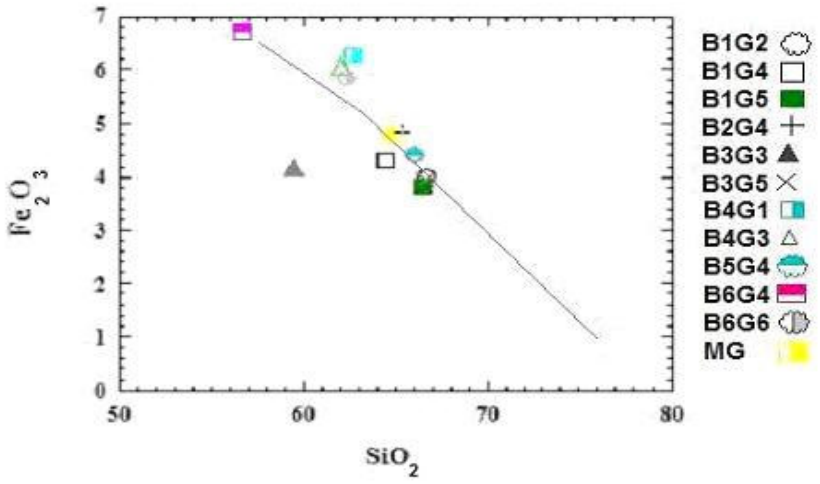

Figure 5.5. Fe_2O_3 vs SiO_2 diagram.

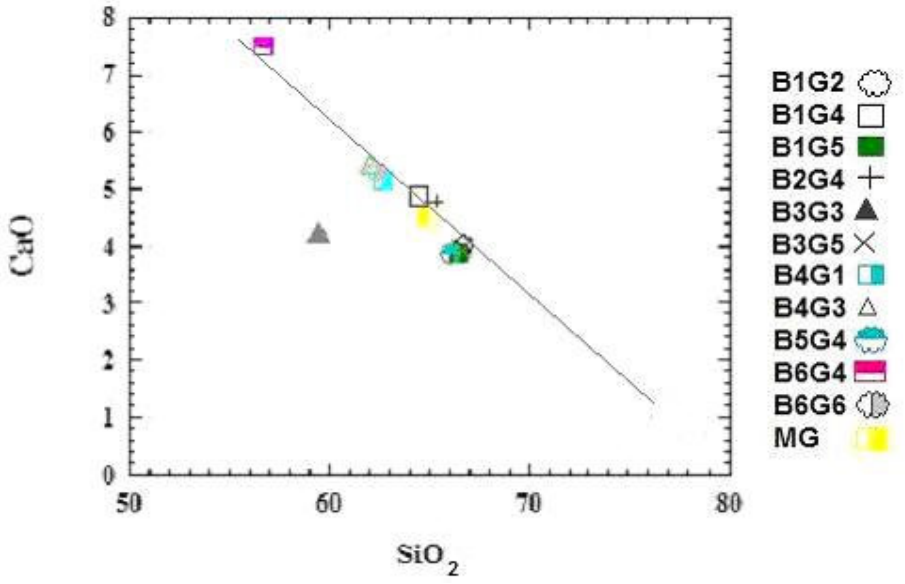

Figure 5.6. CaO vs SiO_2 diagram.

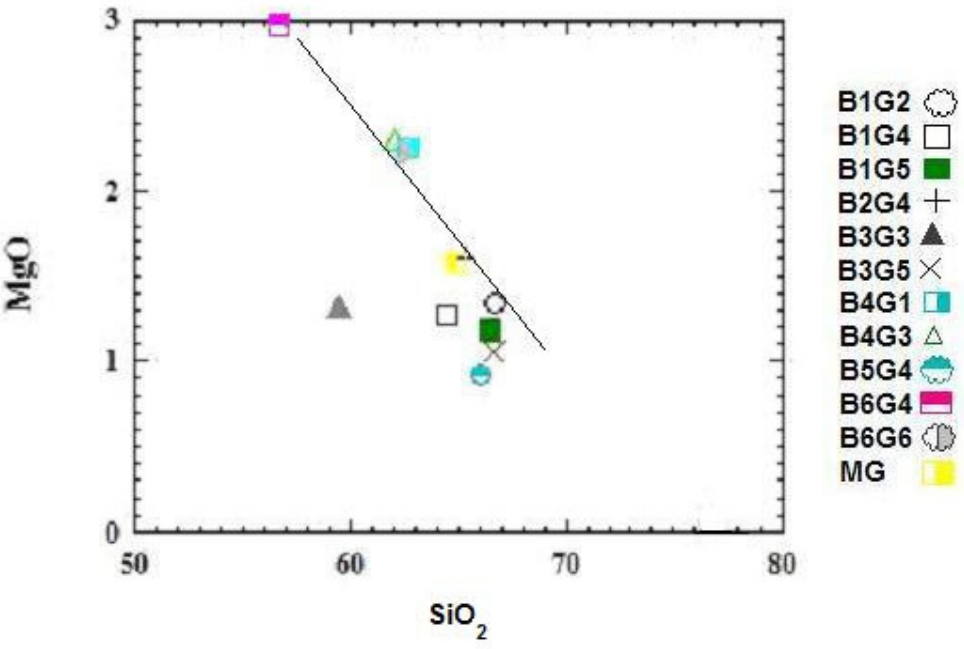

Figure 5.7. MgO vs SiO_2 diagram.

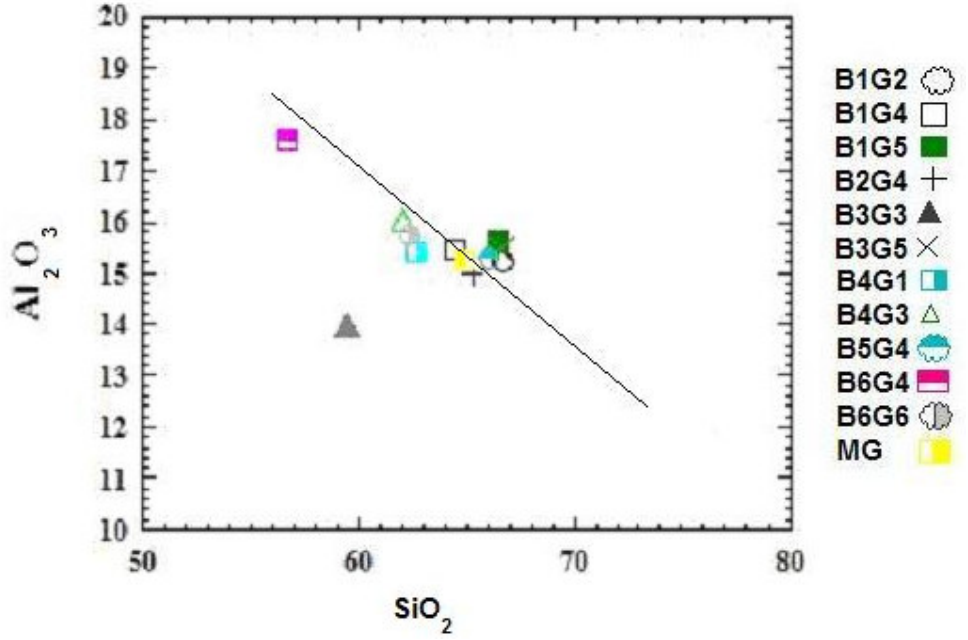

Figure 5.8. Al_2O_3 vs SiO_2 diagram.

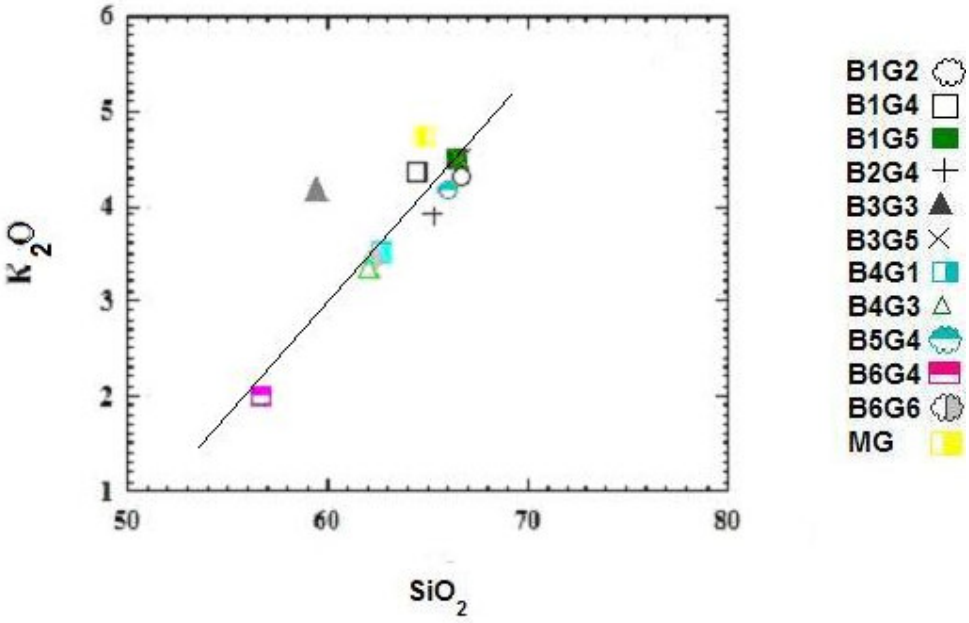

Figure 5.9. K_2O vs SiO_2 diagram.

Only Na_2O vs Si_2O diagram (Figure 5.10) doesn't give any specific trend. Only a slight decrease in Na_2O content is observed with increasing silica content. Since Na is related with plagioclase, it should have been increased with silica. This opposite trend may be because of two reasons; either Na_2O is controlled by hornblende rather than plagioclase, or plagioclases crystallized in early stages, and in late stages K-feldspar is crystallized rather than plagioclase (Yohannes, 1993).

Increase in SiO_2 content with decreasing TiO_2 value (Figure 5.12), also means that the main early crystallizing phases are either sphene or opaque minerals (Fe-Ti oxides).

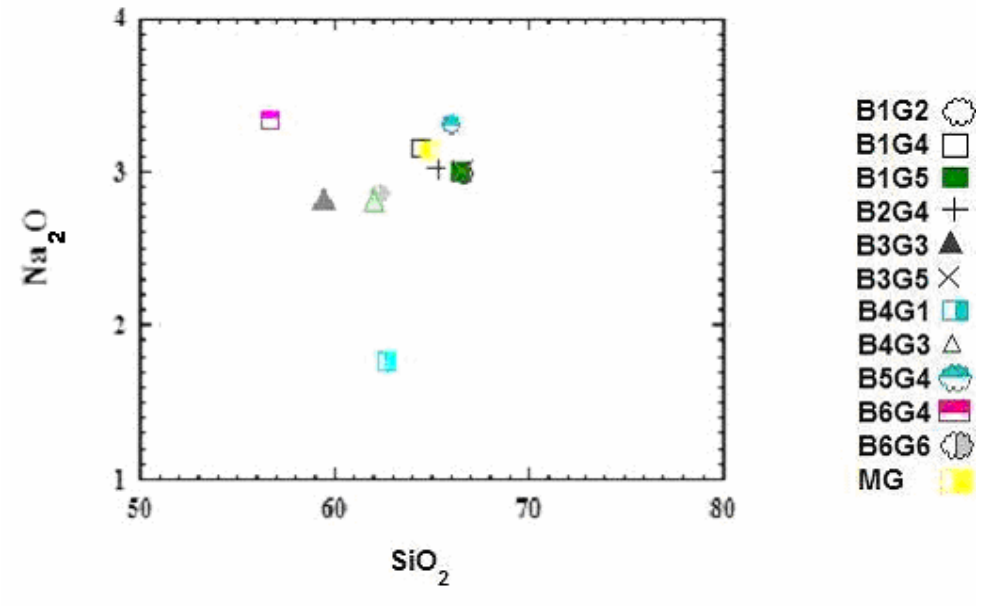

Figure 5.10. Na_2O vs SiO_2 diagram.

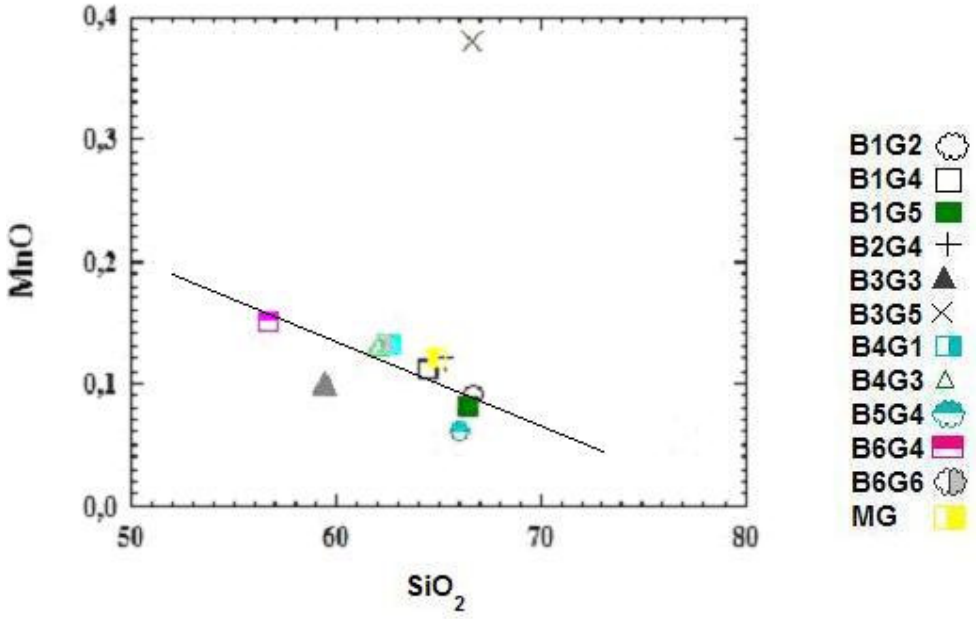

Figure 5.11. MnO vs SiO_2 diagram.

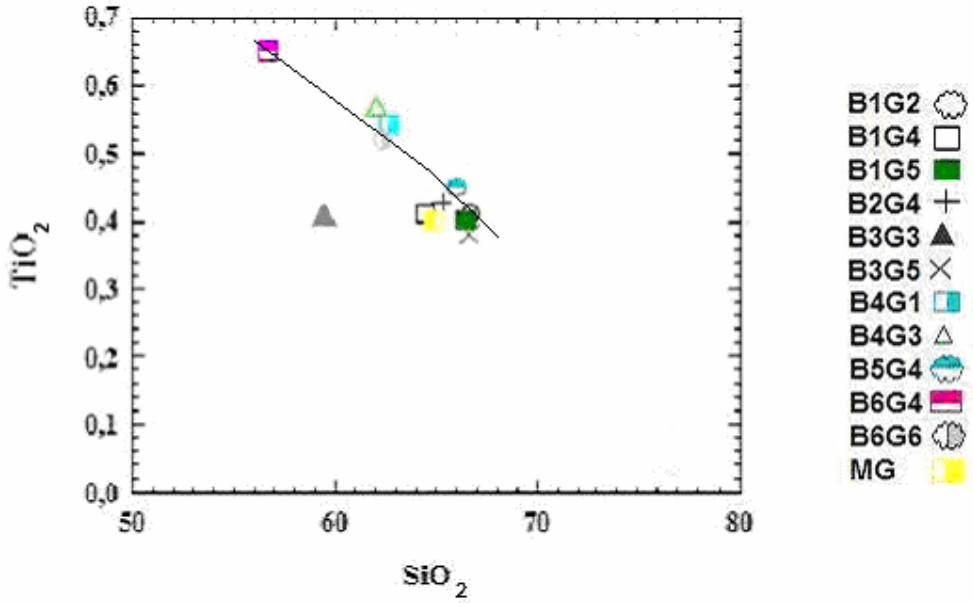

Figure 5.12. TiO_2 vs SiO_2 diagram.

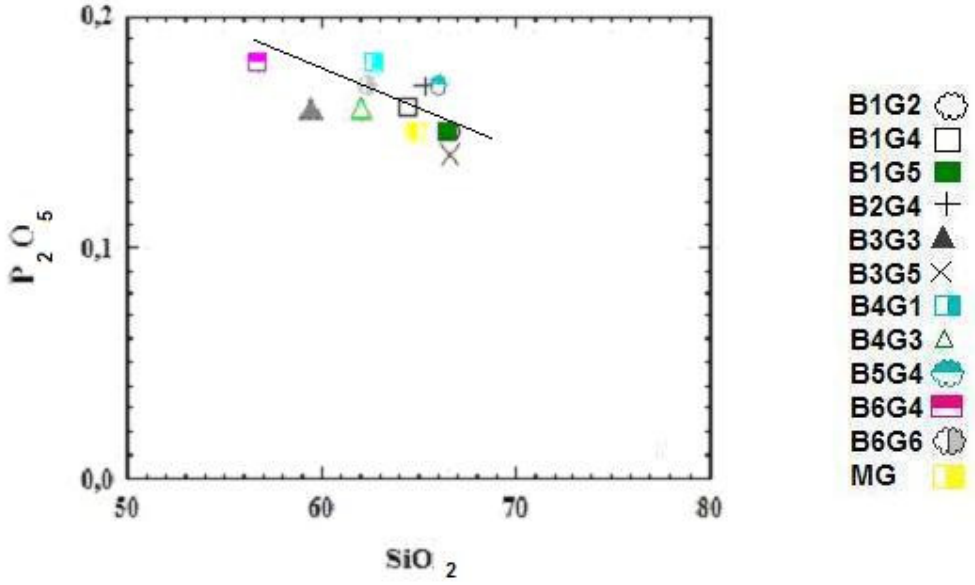

Figure 5.13. P_2O_5 vs SiO_2 diagram.

5.3.2. MAGMA MIXING

Magma mixing is the process in which two magmas of different composition blend to form a single, more or less homogeneous derivative magma (Raymond, 2001). The composition of the derivative magma depends on the amounts of parent magmas relative to each other.

The linear pattern of major oxides could be an evidence for magma mixing. Also for this purpose, trace element versus CaO diagrams are used. Nb, Sr, and Zr vs CaO diagrams (Figures 5.14-16) show a nearly convex upward curve, which means that compositions of enclaves and granites are distinct and this case explains magma mixing according to Poli and Tomassini (1991). In the case of Beypazarı Granitoid and enclaves, magma mixing process is a simple process comprising two parental magmas.

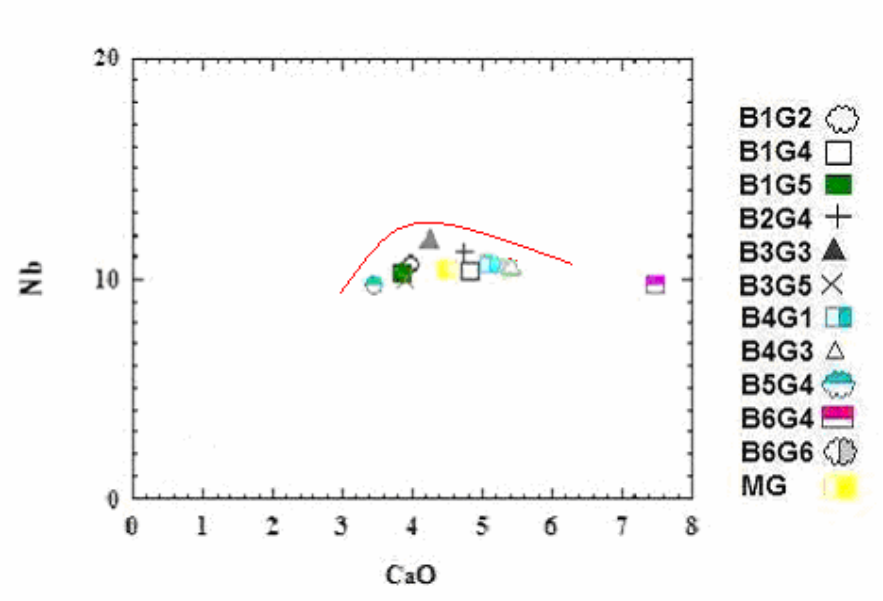

Figure 5.14. Nb vs CaO diagram.

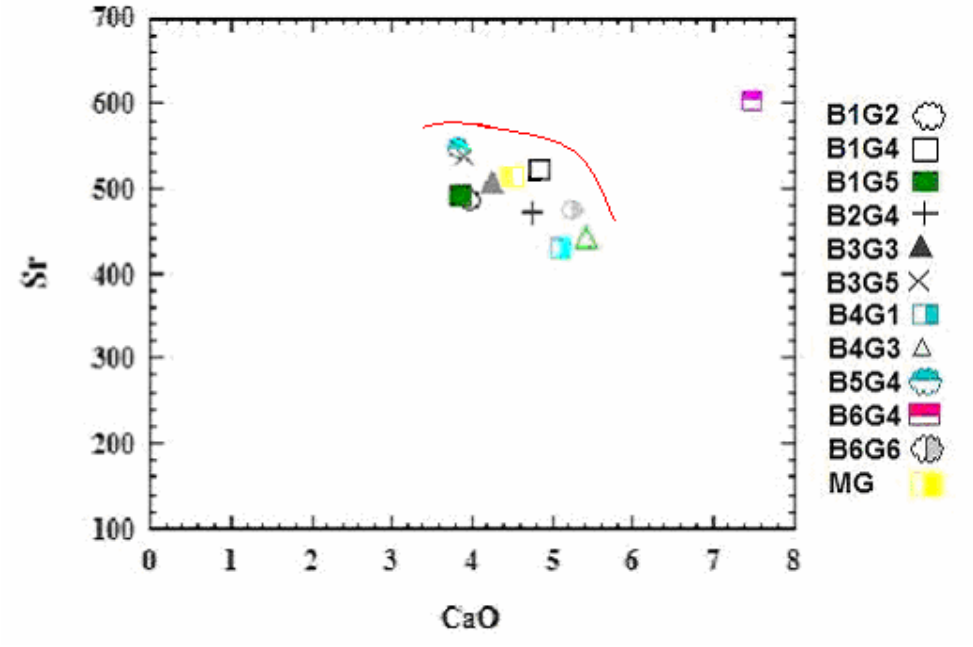

Figure 5.15. Sr vs CaO diagram.

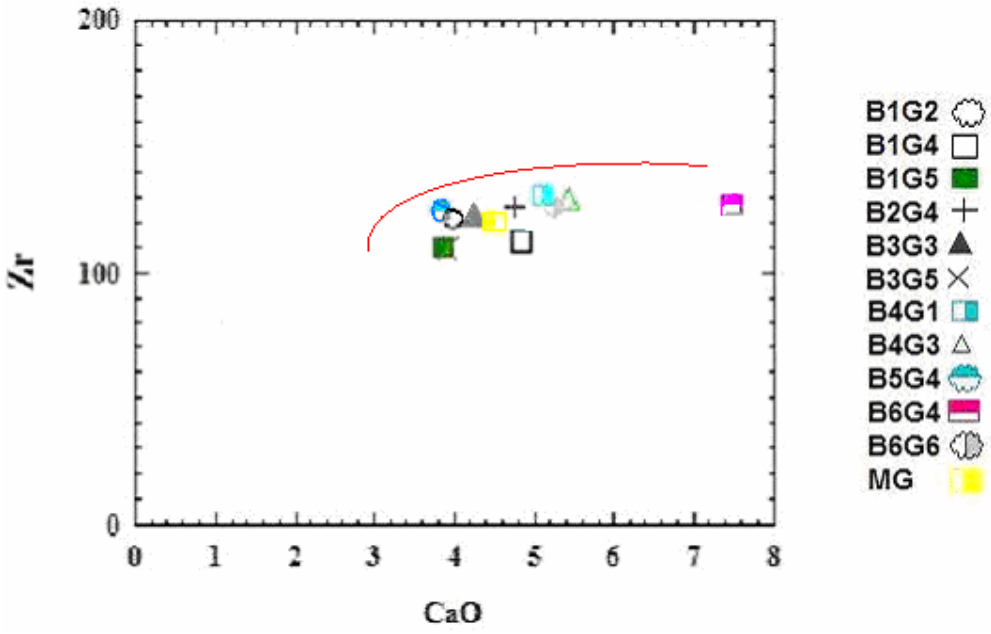

Figure 5.16. Zr vs CaO diagram.

5.3.3. ASSIMILATION

Magmas in magma chamber, or in their path during rising in the mantle or lower crust may melt, dissolve or react with wall rocks. For melting, high temperature is needed and for dissolution, the magma must be undersaturated in components to be dissolved, so these cases are not common. But reaction is common since it involves conversion of wall rock phases compatible with those crystallizing from the magma (Raymond, 2001). Trace element variations may be a clue for understanding effects of assimilation if equilibrium between assimilant and precipitated minerals is not reached (Mc Birney and Noyes, 1979).

U vs Th diagram (Figure 5.17) is used to realize the assimilation of wall rock. The scattered view of graph is an explanation for involvement of wall rock material (Mc Birney and Noyes, 1979).

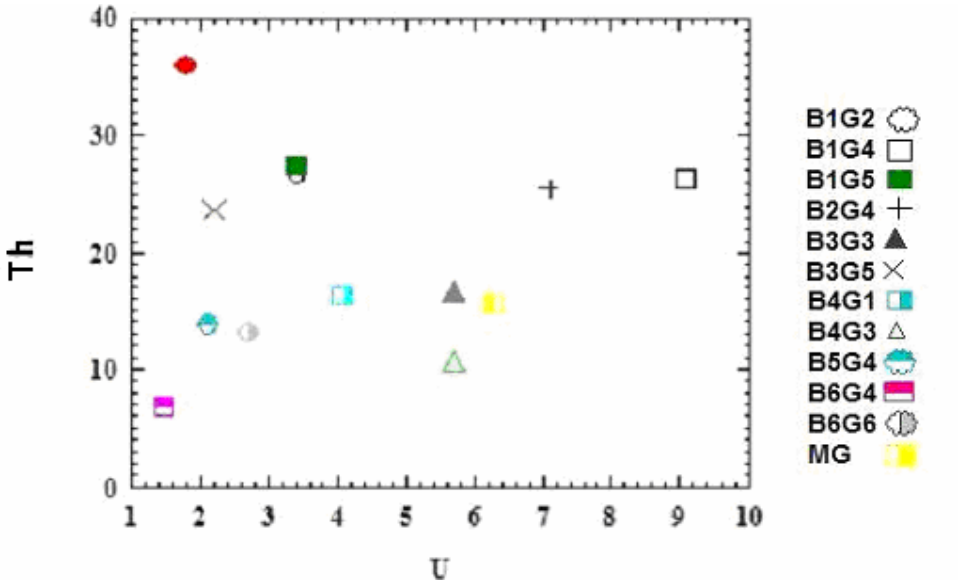

Figure 5.17. Th vs U diagram.

5.4. RARE EARTH ELEMENT DISCRIMINATION

In this section, several REE diagrams are plotted with different normalizing values. According to chondrite normalized diagram (Figure 5.18), the rare earth elements are enriched.

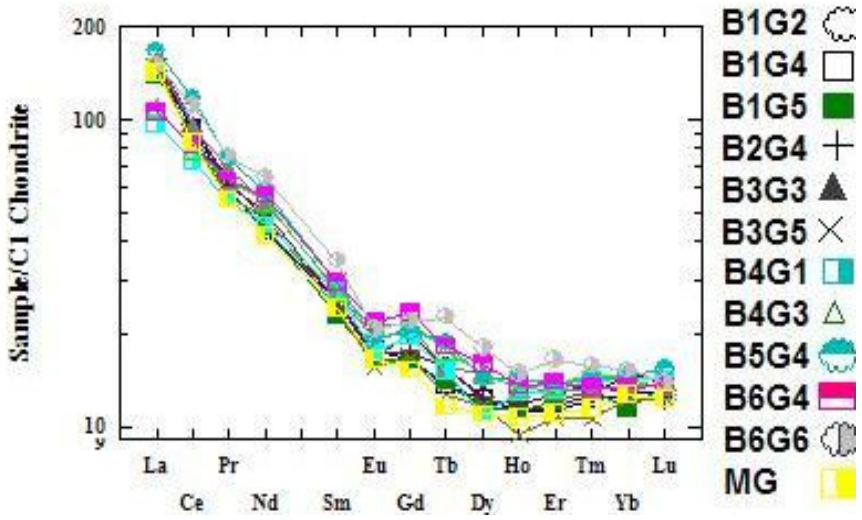

Figure 5.18. Condrite normalized REE discrimination diagram (After Taylor and Mc Lennon, 1985).

On the continental crust-normalized spider diagram the Beypazarı Granitoid shows a trend nearly close to unity (Figure 5.19), which means that the granites may be of continental crustal origin.

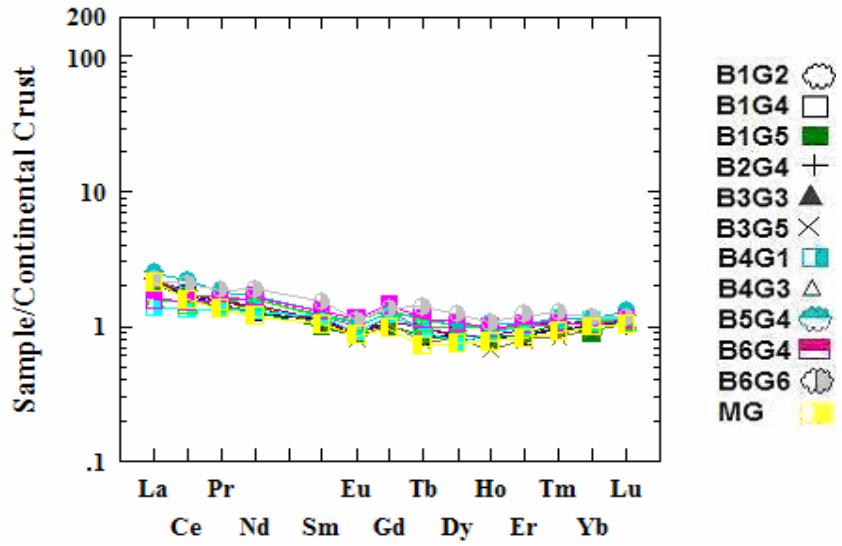

Figure 5.19. Continental crust normalized REE discrimination diagram(After Taylor and Mc Lennon, 1985).

However, the granitoids are enriched relative to lower continental crust (Figure 5.20).

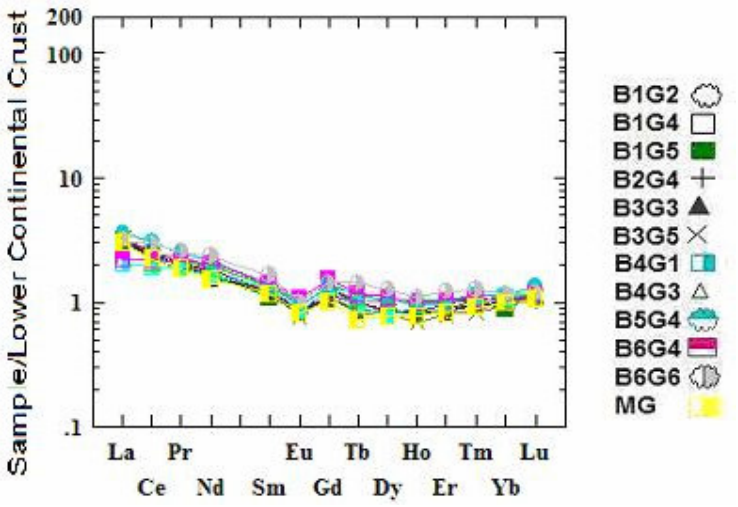

Figure 5.20. Lower continental crust normalized REE discrimination diagram. (After Taylor and Mc Lennon, 1985)

According to upper continental crust normalized REE diagram, the samples show a trend close to unity. This means that the granitoids are of upper continental crustal origin (Figure 5.21).

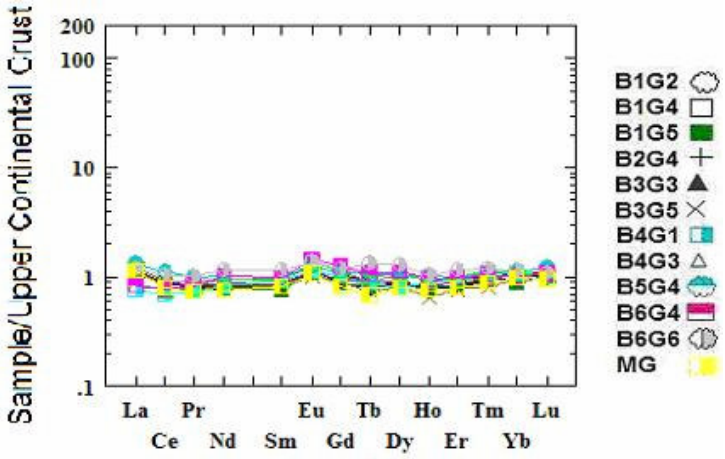

Figure 5.21. Upper continental crust normalized REE discrimination diagram (After Taylor and Mc Lennon, 1985).

When all REE discrimination diagrams are examinated, it is understood that, the Beypazarı Granitoid is originated from upper crust part of continental crust.

5.5. MAJOR OXIDE TECTONIC DISCRIMINATION

In order to define the tectonic environment of emplacement properly, a classification technique with well-defined boundries should be used. Therefore, Maniar and Piccoli (1989) discrimination diagrams are used to study the major oxide classification of this data.

As mentioned before, Maniar and Piccoli (1989) subdivided the granitoids according to their tectonic environment: (1) island-arc granitoids (IAG), (2) continental-arc granitods (CAG), (3) continental-collision granitoids (CCG), (4) post-orogenic granitoids (POG), (5) continental epeirogenic uplift granitoids (CEUG), (6) rift-related granitoids (RRG), and (7) oceanic plagiogranite (OP). Those subdivisions belong to two main groups; orogenic granitoids, IAG, CAG, CCG, POG, and anorogenic granitoids, CEUG, RRG, and OP (Yohannes, 1993).

Maniar and Piccoli (1989) discrimination diagrams are integrated using the Shand's index (Shand, 1951).

There are three steps for the discrimination of granites by using the discrimination diagrams of Maniar and Piccoli (1989). The first step is to discriminate oceanic plagiogranite (OP) from others. For this purpose K_2O vs SiO_2 diagram (Figure 5.22) is used. The diagram is based on the idea that oceanic plagiogranites (OP) have low content of K_2O which corresponds to minor occurence of K-feldspar. The second step is to discriminate granites between three groups; group 1 [island-arc granitoids (IAG), continental-arc granitods (CAG), continental-collision granitoids (CCG)], group 2 [continental epeirogenic uplift granitoids (CEUG), rift-related granitoids (RRG)], group 3 [post-orogenic granitoids (POG)]. For this discrimination step three diagrams are available. Al_2O_3 vs SiO_2 diagram is useful for SiO_2 values greater than 70 wt%, however, analysed samples contain less

than 70 % silica, so this diagram is not used. $FeO^T/[FeO^T+MgO]$ vs SiO_2 diagram (Figure 5.23) is good for lower SiO_2 values. AFM and ACF (Figure 5.24, 5.25) is useful for discrimination of group 1 and group 2. In all discrimination diagrams, group 3 field which covers the post-orogenic granitoids (POG) occurs.

For the third step there are two possible ways to follow: (i) discrimination between group 1 granitoids [island-arc granitoids (IAG), continental-arc granitods (CAG), continental-collision granitoids (CCG)] using Shand's Index (Shand, 1951 in Maniar and Piccoli, 1989) (Figure 5.26). If $A/(C+N+K) < 1.05$ granitoids are arc granitoids, not continental-collision granitoids (CCG). If $A/(C+N+K) > 1.15$ granitoids are CCG and if $1.05 < A/(C+N+K) < 1.15$, no discrimination is possible. (ii) discrimination between group 2 granitoids (continental epeirogenic uplift granitoids (CEUG), rift-related granitoids (RRG)) using TiO_2 vs SiO_2 diagram, where rift-related granitoids (RRG) have lower TiO_2 content. This discrimination can be made only for SiO_2 values greater than 60 wt%.

Discrimination of 12 samples from main granitoid body is performed as follows:

For the first step, K_2O vs SiO_2 diagram (Figure 5.22) is used as mentioned above. None of samples lie in the oceanic plagiogranite (OP) region.

Next step is discrimination of granites between three groups. Since SiO_2 values are less than 70% Al_2O_3 vs SiO_2 diagram is not used.

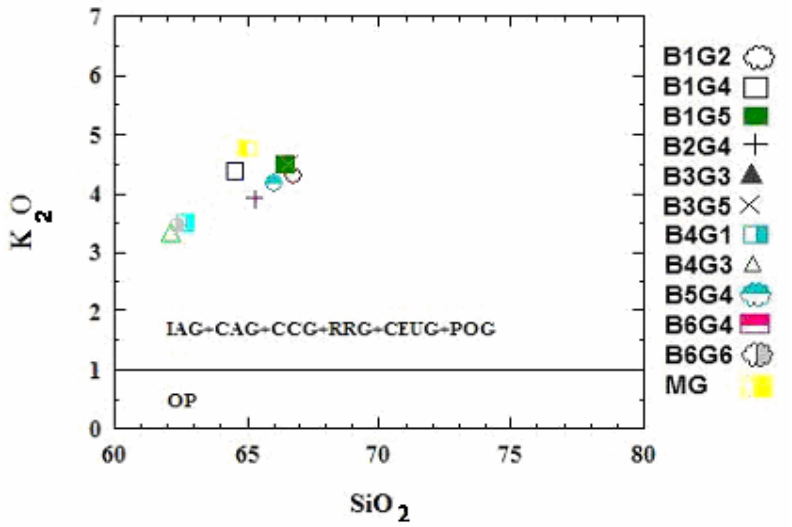

Figure 5.22. K_2O vs SiO_2 diagram (wt%) (After Maniar and Piccoli, 1989).

Then samples are plotted on $FeO^T/[FeO^T+MgO]$ vs SiO_2 diagram (Figure 5.23). According to this plot all granite samples fall in the region IAG+CAG+CCG.

According to the AFM (Figure 5.24) and ACF (Figure 5.25) diagrams, the samples belong to group 1 (IAG+CAG+CCG).

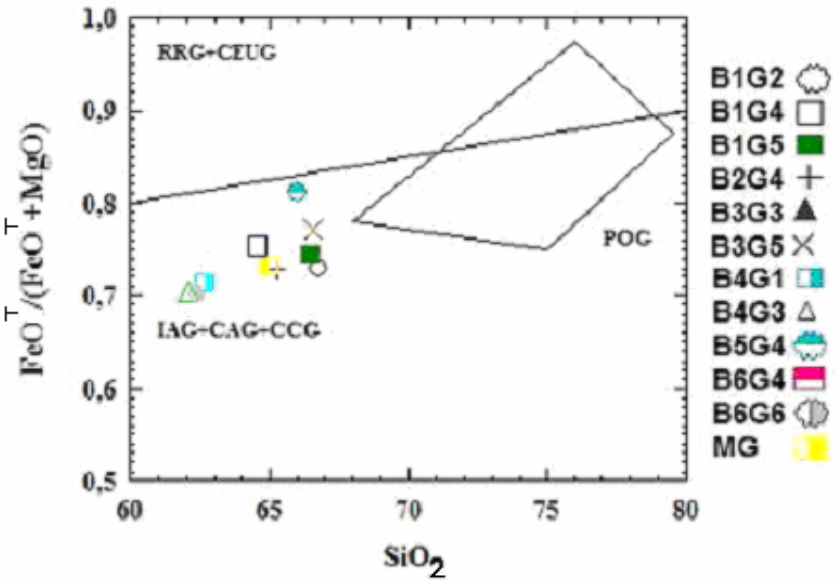

Figure 5.23. $FeO^T/[FeO^T+MgO]$ vs SiO_2 diagram (wt%) (After Maniar and Piccoli, 1989).

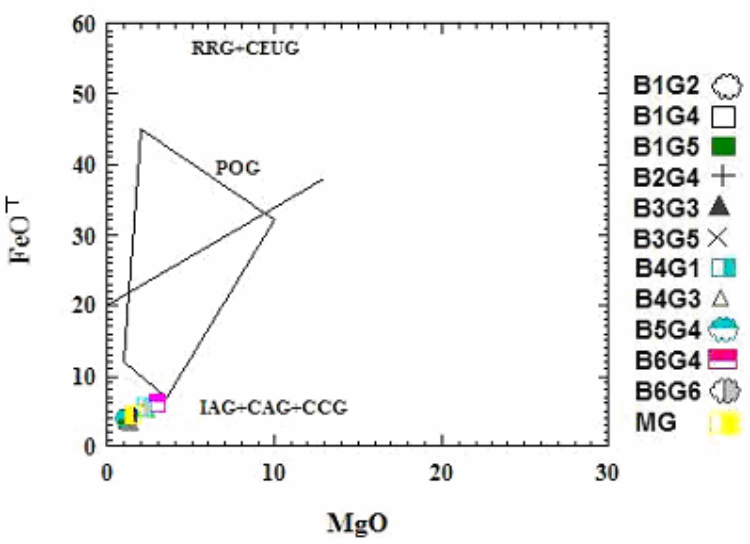

Figure 5.24. FeO^T vs MgO diagram (wt%) (After Maniar and Piccoli, 1989).

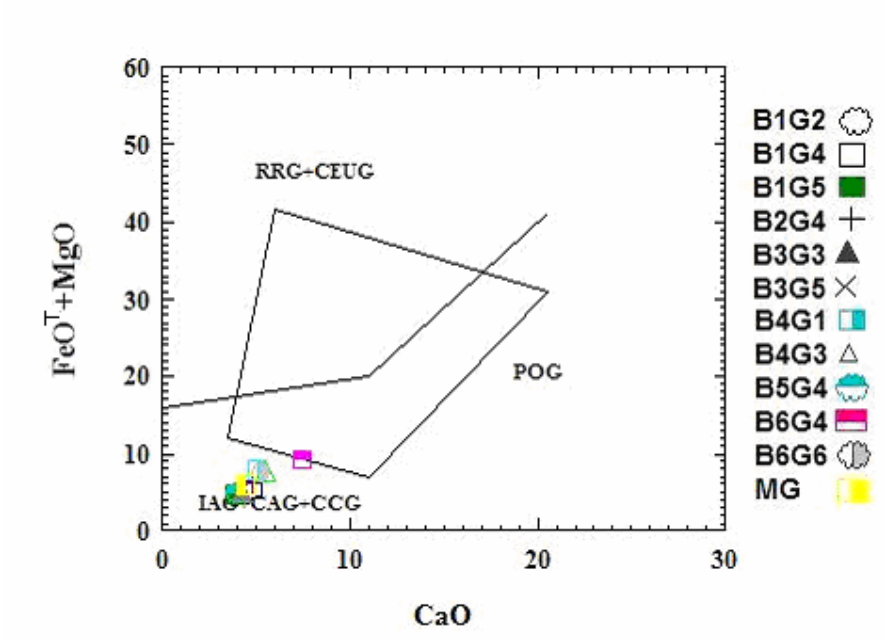

Figure 5.25. (FeO^T+MgO) vs CaO wt(%) diagram (After Maniar and Piccoli, 1989).

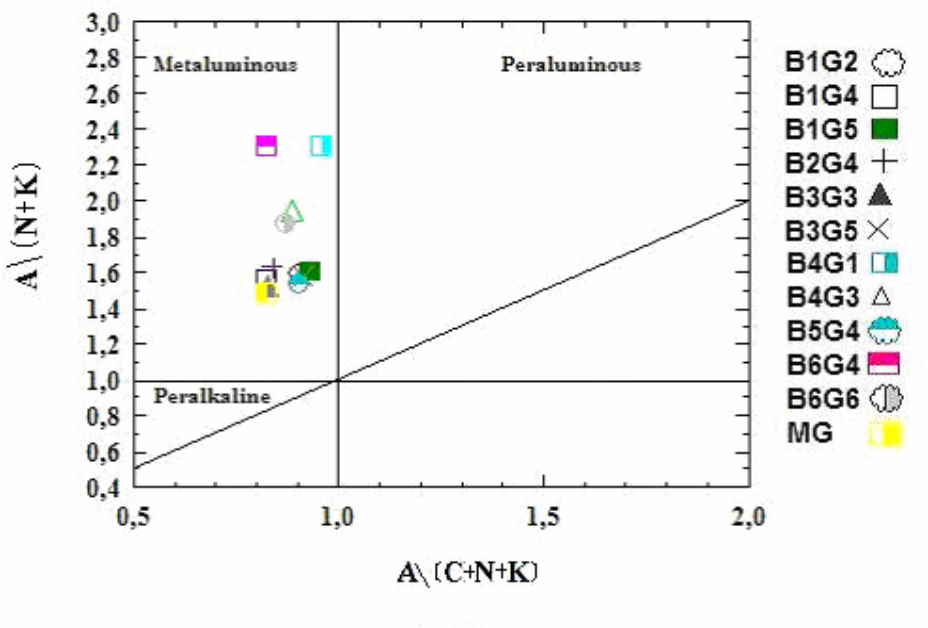

Figure 5.26. A/(N+K) vs A/(C+N+K) diagram (After Maniar and Piccoli, 1989).

In order to subdivide samples of group 1, Shand's Index is useful. By using A/(N+K) vs A/(C+N+K) diagram (Figure 5.26), it is seen that aplite sample is peraluminous, and all other samples are metaluminous in first sense. According to (A/C+N+K) values, all granite samples are arc granitoids, in other words not CCG.

By using major oxide discrimination techniques, it is understood that, granites are arc granitoids, in other words, they are either island-arc granitoids (IAG), or continental-arc granitods (CAG).

5.6. TRACE ELEMENT TECTONIC DISCRIMINATION

Many trace element discrimination diagrams are prepared for determintion of tectonic environment. However, most of those diagrams are available for rocks of basaltic composition, but there are some discrimination diagrams used for granites. Pearce *et al.* (1984) discrimination diagrams play important role in discriminating tectonic settings of granites.

As mentioned before, Pearce *et al.* (1984) classified granitoids into four main groups as, ocean-ridge granitoids (ORG), volcanic-arc granitoids (VAG), within plate granitoids (WPG), and collision granites (COLG).

The first group of discrimination diagrams used by Pearce *et al.* (1984) are trace element vs SiO_2 diagrams that are formulated on the basis of systematic trace element variation between different tectonic settings. WPG and ORG comprises higher amounts of Y relative to VAG, COLG and ORG (Figure 5.27). Rb vs SiO_2 diagram can be used to differentiate WPG and ORG from each other. The same diagram also discriminates VAG from Syn-COLG (Figure 5.28), since latter has high Rb values. WPG have high values of Nb compared to other types (Figure 5.29). Therefore it is useful to discriminate WPG from others. It is nearly impossible to discriminate every tectonic setting from each other by using above discrimination diagrams. For this reason, Pearce *et al*. (1984) used two other diagrams; Nb vs Y and Rb vs (Y+Nb). Especially the latter diagram is a useful diagram to discriminate tectonic settings of granites.

Pearce *et al*. (1984) diagrams fails to interpret the post-collision granites because, their source may be crustal or mantle rocks.

Data of 12 samples are plotted on the Pearce *et al*. (1984) discrimination diagrams mentioned above.

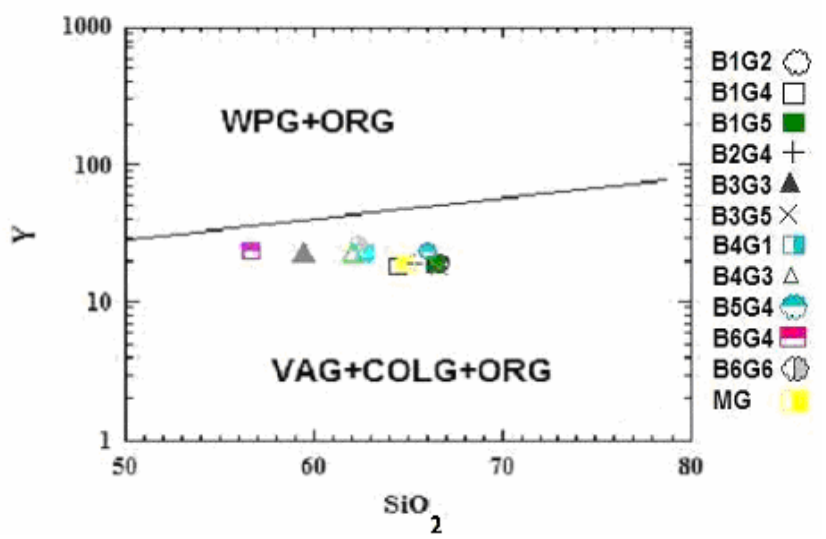

Figure 5.27. Y(ppm) vs SiO_2 (wt%) diagram (after Pearce *et al*. 1984)

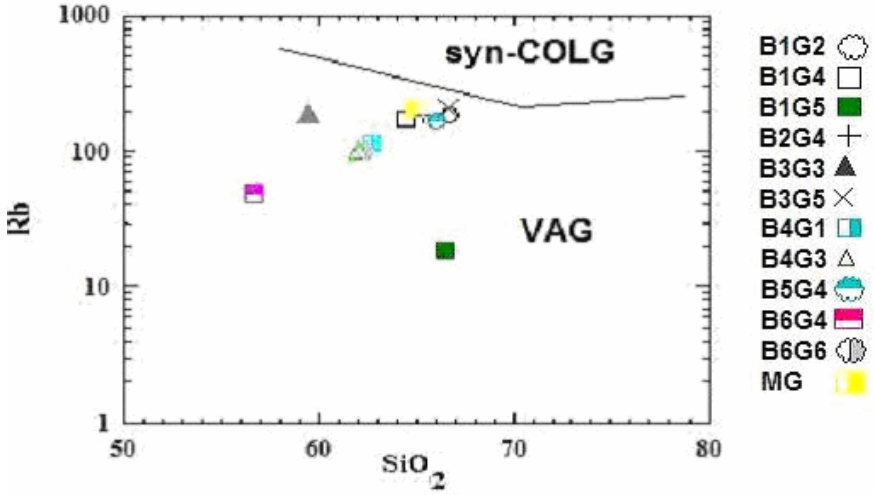

Figure 5.28. Rb (ppm) vs SiO_2 (wt%) diagram (after Pearce *et al*. 1984)

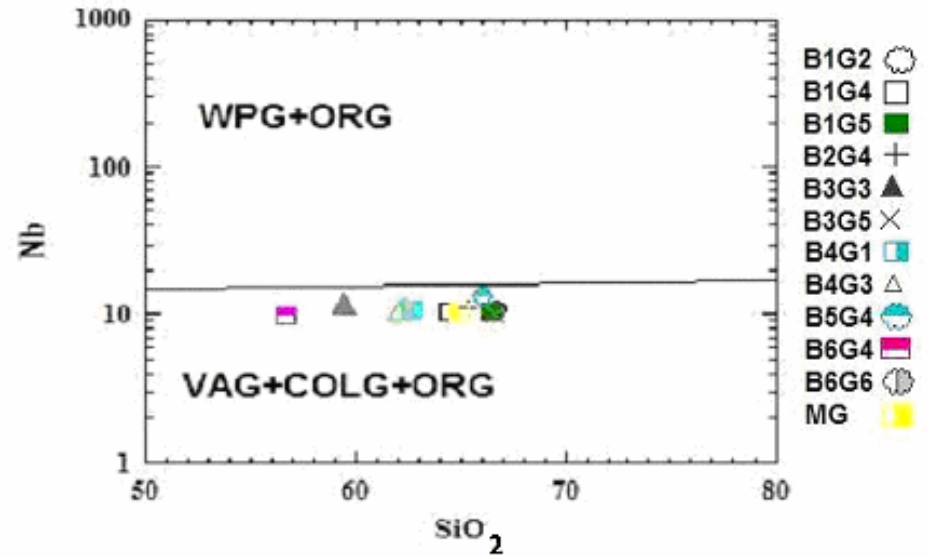

Figure 5.29. Nb (ppm) vs SiO_2 (wt%) diagram (after Pearce *et al*. 1984)

In Figures 5.27 and 5.29 all samples fall in the region volcanic-arc granitoids (VAG), collision granites (COLG), and ocean ridge granitoids (ORG). diagram. However in Figure 5.28, all samples fall in the region of volcanic-arc granitoids (VAG).

According to discrimination diagram group distributed in figure 5.27, main granite of Beypazarı Granitoids is volcanic-arc granitoids (VAG).

When samples are plotted on Nb vs Y diagram (Figure 5.30), it is seen that they fall in the region volcanic-arc granitoids (VAG) and syn-collision granites (syn-COLG). However, all granite samples fall in the volcanic-arc granitoids (VAG) region when plotted to the Rb vs (Y+Nb) diagram (Figure 5.31).

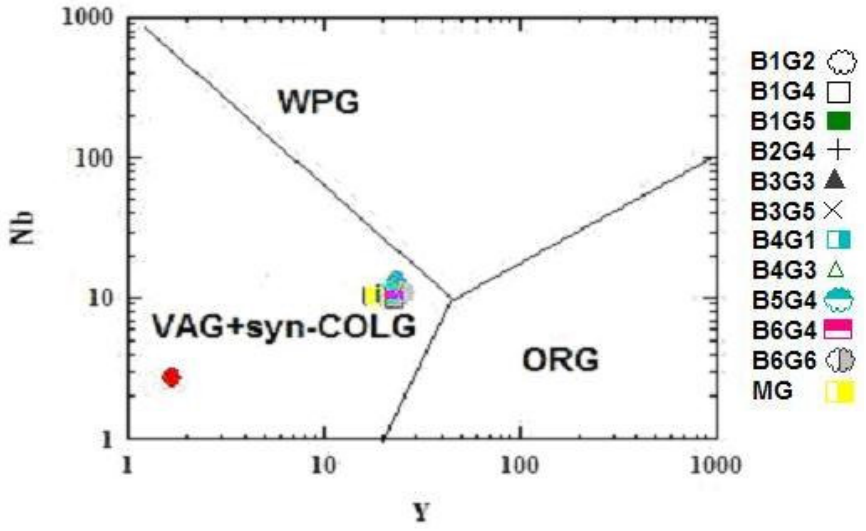

Figure 5.30. Nb vs Y diagram (after Pearce *et al*. 1984).

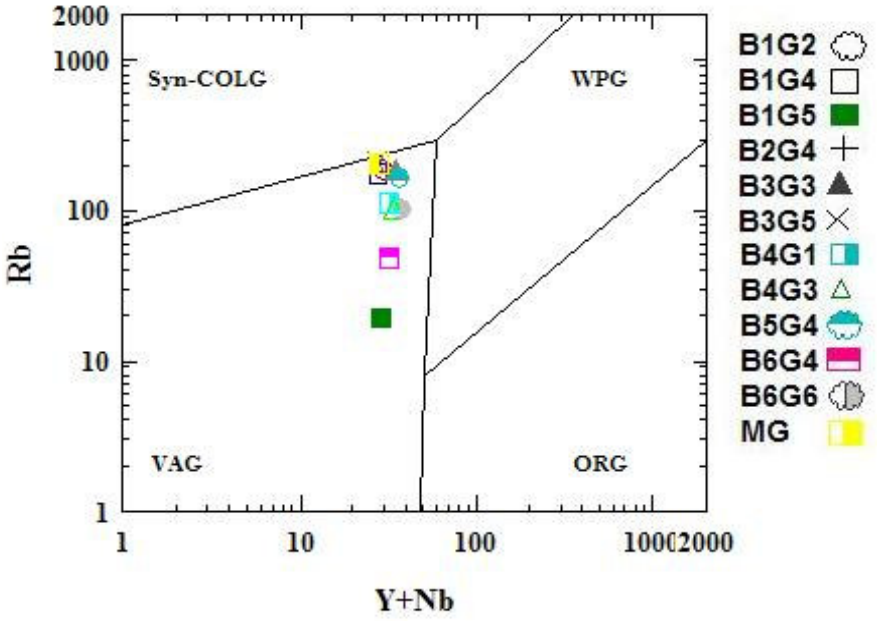

Figure 5.31. Rb vs (Y+Nb) diagram (after Pearce *et al*. 1984).

5.7. SPIDER DIAGRAMS

In this section, ocean ridge granitoid normalization values are used (Table 5.4). Trace element patterns, give idea about source and magmatic processes. Difference in elemental patterns are important since mobile incompatibles (Sr, K, Ba, Rb) go to melt and immobile compatibles are kept in the subducting slab (Figure 5.32).

Table 5.4. ORG Normalizing Values (Pearce *et al.* 1984).

Element	Normalizing Values
K_2O	0,4
Rb	4
Ba	50
Th	0,8
Ta	0,7
Nb	10
Ce	35
Hf	9
Zr	340
Sm	9
Y	70
Yb	80

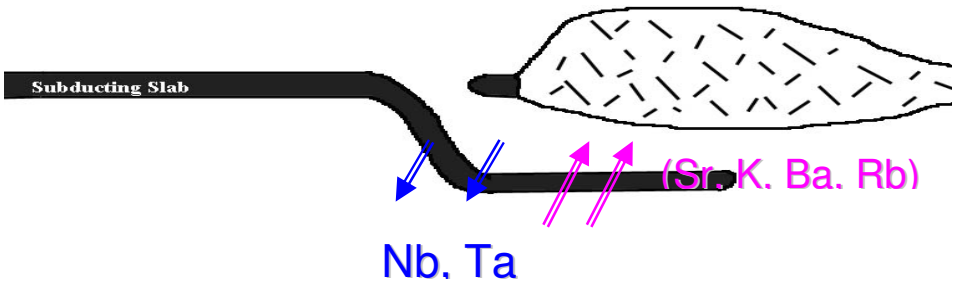

Figure 5.32. Behaviours of incompatible elements (N. Güleç "Geochemistry" lecture notes, 2001).

According to Pearce *et al.* (1984), spider diagrams for ocean-ridge granitoids (ORG) give a flat pattern close to unity. However, spider diagrams for volcanic arc granites (VAG) give inclined pattern due to enrichment in LILE (K, Rb, Ba) and Th relative to HFSE (Ta, Zr, Y, Yb). Little enrichment in Rb is observed and continental margin granitoids have higher enrichment of LILE than island arc granitoids (Figure 5.33). Slightly inclined pattern however indicates within plate granitoids (WPG), and depletion in Ba indicates mantlesource. It is complicated to observe crustal source, it can be observed by its gentle slope between Ba, Ta, Th unlike other granites. Similar to VAG, collision granites (COLG) show inclined pattern and exceptionally high Rb in syn-collision granites (SYN-COLG).

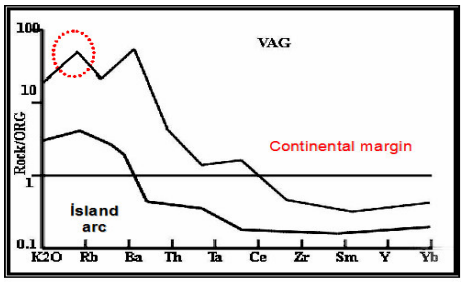

Figure 5.33. Spider diagram for VAG (after Pearce *et al*. 1984).

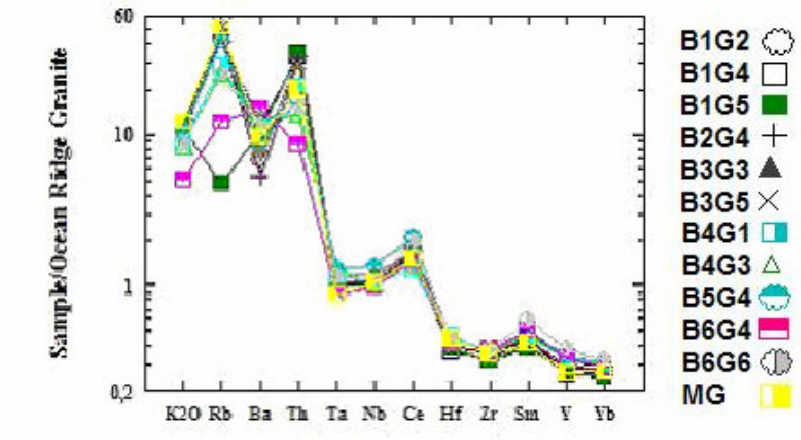

Figure 5.34. Ocean Ridge Granite (ORG) normalized spider diagram for Beypazarı Granitoid (after Pearce *et al*. 1984).

The ORG-normalized spider diagram of Beypazarı Granitoid shows inclined pattern which means the granitoids are volcanic arc grantoids. Little enrichment in Rb, high enrichment of LILE indicates continental origin. Therefore, the Beypazarı granitoids are volcanic arc granitoids (VAG) of continental origin according to spider diagram (Figure 5.39).

5.8. CHEMICAL CLASSIFICATION OF GRANITOIDS

Granitoids are of four types according to chemical criteria, I-type, S-type, A-type and M-type. I-type grantoids form by partial melting and differentiation of igneous rocks. S-type granitoids form by partial melting and/or differentiation of sedimentary rocks. A-type granitoids are first proposed by Collins *et al.* (1982) for the Upper Devonian granitoids in the Lachland Fold Belt in Australia. A-type stands for alkaline, anhydrous, anorogenic. M-type granitoids form by partial melting of metamorphic rocks. The Beypazarı Granitoid is metaluminous (Figure 5.26), variation diagrams give linear trends, Na_2O+K_2O is low, Ni, V, Co, Cr are high and Nb, Ce, Zn, Zr are lower. Volcanic arc granitoids from continental margins corresponds to I-type according to Pearce *et al.* (1984). Quartz-monzonite, granodiorite and granite are common and biotite and hornblende are the dominant mafic minerals. Therefore, the Beypazarı Granitoid is I-type granitoid.

CHAPTER 6

DISCUSSION

The petrochemical and petrological data suggest that the granitoid of the present study is calcic, metaluminous, I-type granite, and granodiorite-diorite.

REE diagrams indicate that the studied granitoids were originated from the upper continental crust (Figure 5.21). According to major oxide and trace element diagrams, Beypazarı Granitoid is volcanic-arc granitoid.

One of the typical features of Beypazarı Granitoid is mafic microgranular enclaves. Didier (1973) defined "enclave" as "bodies of material totally enclosed within and differing in some way from the otherwise fairly homogeneous igneous rock in which it is found." Depending on their chemical and mineralogical composition , enclaves are of various types (Didier, 1973, 1987; Eberz and Nicholls, 1990). Genetically, there are two types of enclaves. In the first category, enclaves are fragments with a common origin with the main igneous body. Segregations and restites are examples for this category. Segregation of minerals in the magma during early or late stages of crystallization cause segregations and residues left over from partial melting of the source material produce restites or they may be products of mingling of a different. The second category of enclaves are the "xenoliths", the foreign materials having no common origin with the main igneous rock. Xenoliths can be fragments of host rocks which are taken by magma during its ascent magma.

According to this study and to Yohannes (1993), the evidences such as sharp contact relationship, lack of complex or reverse zoning of plagioclase and the absence of any textural criteria, such as foliated fabric, or granoblastic texture suggest restitic (including magma mixing) or seggregation origin. Similary, lack of

evidences for xenoliths similar to wall rocks suggests to ignore xenolitic (accidental inclusion) origin. Therefore, the overall evidences show that the enclaves are probably magma mixing product and the enclaves observed resemble the first category of enclaves mentioned by Didier (1973, 1987) and Eberz and Nicholls (1990).

Although, it is not directly observed in the study area, the granite intruded the Tepeköy metamorphics of Sakarya Composite Terrane (Göncüoğlu *et al.* 2000), by this its intrusion should be younger than this unit. Pebbles of Beypazarı Granitoid are observed in the basal conglomerates of Palaeocene sediments according to Helvacı and Bozkurt (1994). Therefore, age of granitoids are younger than Early Mesozoic, older than Paleocene, probably Late Cretaceous (Helvacı and Bozkurt, 1994).

The study area is located in Central Sakarya Area where three main Alpine tectonic units juxtapose. These are; the Sömdiken Metamorphics representing the Tauride-Anatolides, the Sakarya Composite Terrane and the ophiolites of the İzmir-Ankara Zone (Figure 6.1).

The geodynamic scenario commonly accepted by Şengör and Yılmaz (1981) and Göncüoğlu, (1997) is that the İzmir-Ankara-Erzincan Ocean had closed by northward subduction. If this interpretation is valid, the studied area must be located at the active margin of the İzmir-Ankara-Erzincan Ocean, above the northward subducting oceanic lithosphere (Figure 6.2). This would explain the magmatic arc character of the studied Beypazarı Granitoid, so that the possible mechanism of Beypazarı Granitoid is the north-dipping subduction of Neo-Tethyan northern branch under Sakarya continent.

In this model, the melting started in the upper mantle above the subducting slab, but it is followed by melting of the lower crust and finally the upper crust which resulted in the formation of the Beypazarı Granitoid.

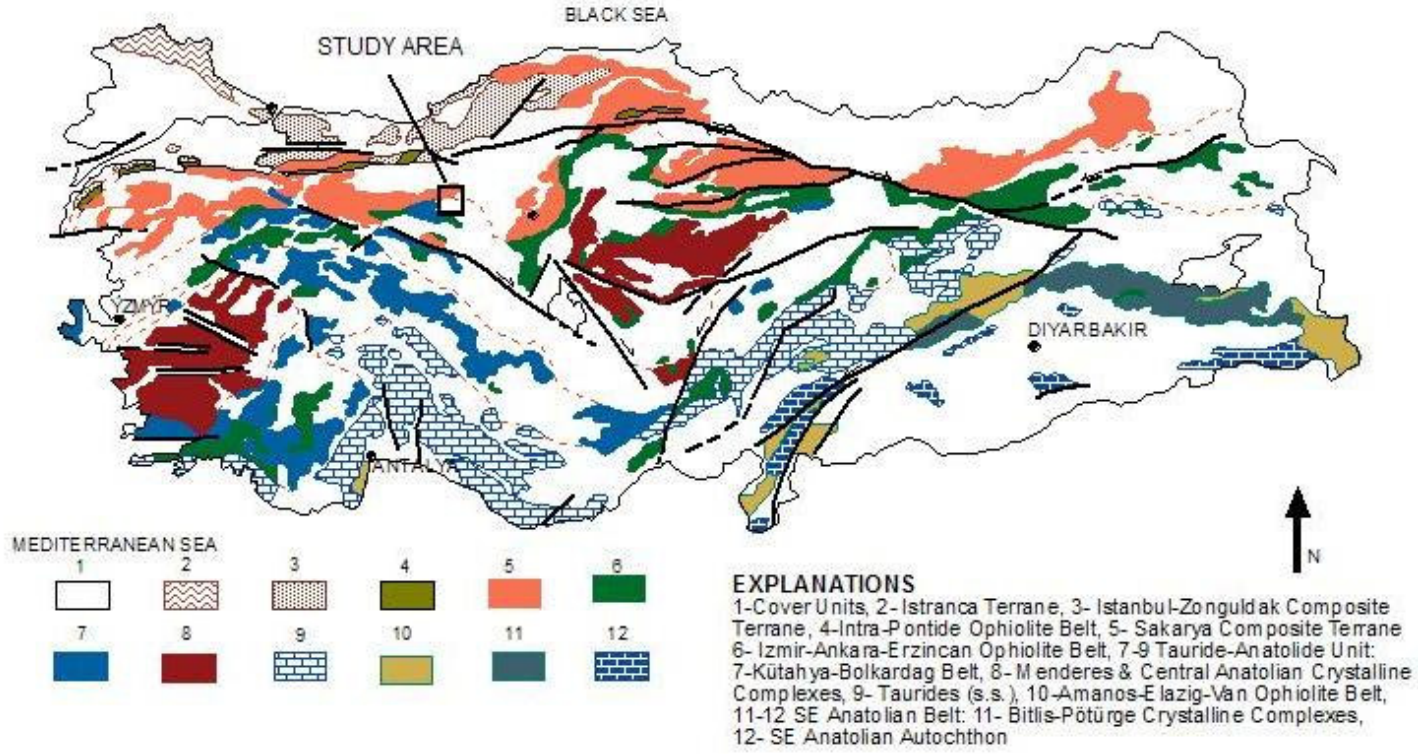

Figure 6.1. Terrane map of Turkey (Göncüoğlu, 1997).

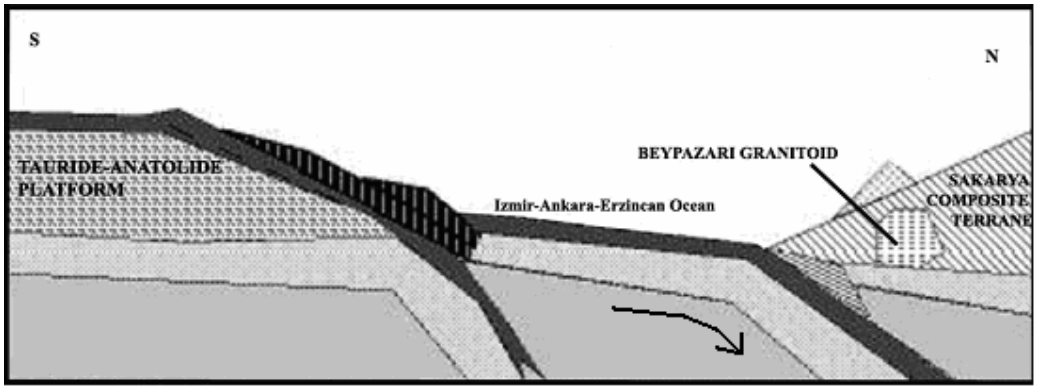

Figure 6.2. The northward subduction of İzmir-Ankara-Erzincan Ocean under Sakarya Composite Terrane (Göncüoğlu, *et al*, 2000).

The granite magmatism can be related to the Galatian Magmatic Arc which is located to the northwest of Beypazarı Granitoids. In order to connect them, a tectonic model can be proposed where first, a high angle subduction before granitoid intrusion takes place probably before Early Cretaceous and then a low angle subduction takes place during formation of Galatian Magmatic Arc with successive granitoid intrusions (Yohannes, 1993), (Koçyiğit *et al.* 2003, and references therein). This model can be applied to the granitoids of the study area.

According to Figure 6.3, Beypazarı Granitoid studied by Helvacı and Bozkurt (1994) is similar to the granite studied in this thesis. As it is the case with the studied granitoid, the Beypazarı Granitoid is calc-alkaline, calcic and metaluminous and belongs to volcanic arc tectonic setting.

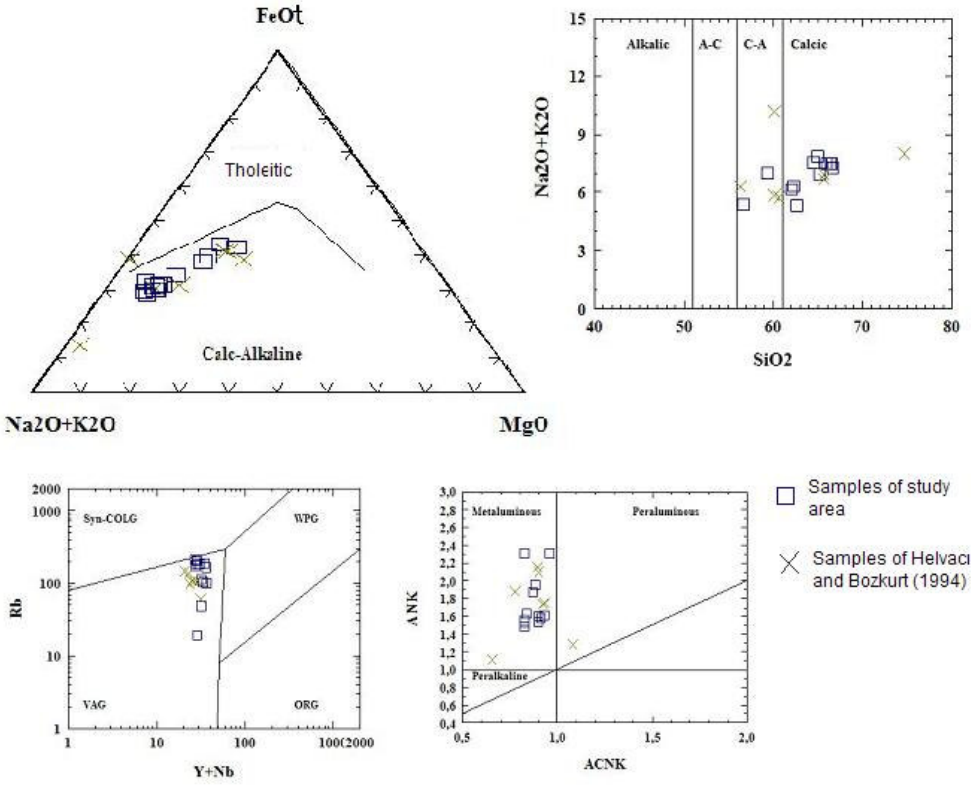

Figure 6.3. Comparison between samples of Helvacı and Bozkurt (1994) and samples of this study area.

CHAPTER 7

CONCLUSION

The petrogenesis of Beypazarı Granitoid is examined with the assistance of petrochemical, petrological and geological studies.

Geologically the Beypazarı Granitoid is located within the Sakarya Composite Terrane, close to the İzmir-Ankara suture belt. The studied granitoid intruded the Tepeköy Metamorphics of the Sakarya Composite Terrane and is unconformably overlain by Palaeocene-Eocene clastics.

Petrographically, the Beypazarı Granitoid is coarse grained, holocrystalline and hypidiomorphic. When the point-counting analysis for samples are located on the QAP Streckeisen triangular diagram (Streckeisen, 1976), it is seen that the samples belong to the "granite", "alkali-feldsar granite", and the "quartz-rich granitoid" fields. The samples corresponding to the region "Alkali-feldspar granite" represent aplite dykes. The granitoid is composed of quartz, alkali feldspar, plagioclase, pyroxene, hornblende, minor amounts of biotite, zircon, sphene, apatite, zeolite, opaque minerals, and calcite and sericite as alteration products.

Geochemical data indicate that the granitoids are calc-alkaline, metaluminous, and I-type with mafic microgranular enclaves; charactristic for magma mixing. The tectonic discrimination diagrams suggest that they are arc granitoids. The source of granitoids could be the fractional crystallization of upper-crust derived magma.

The granitoid is formed above the northward subducting İzmir-Ankara oceanic plate and related to the Galatean magmatic arc.

Since this study is performed with limited data, for better evaluation, more samples should be analysed for major oxide, trace element and rare earth element compositions; isotope ratios and absolute age determination should be considered.

REFERENCES

Altıner, D., Koçyiğit, A., Farinacci, A., Nicosia, U. and Conti, M.A., 1991. "Jurassic-Lower Cretaceous stratigraphy and paleogeographic evolution of north western Anatolia (Turkey)", Geologica Romana, v. 27, p. 13-80.

Chappel, B.W. and White, A.J.R., 1974. "Two contrasting granite types", Pacific Geology, v.8, 173-174.

Collins, W.J., Bearns, S.D., White, A.J.R. and Chappel, B.W., 1982. "Nature and origin of A-type granites with particular reference Southeastern Australia", Cont. Miner. Petrol. v.10, p.189-200.

Cox, K. G.; Bell, J. D. and Pankhurst, R. J, 1979. "The Interpretation of igneous Rocks", George Allen & Unwin, London, p. 450.

Didier, J., 1973. "Granites and their enclaves", Coll. Developments in petrology, Elsevier, Amsterdam, p. 393.

Didier, J., 1987. "Contribution of enclave studies to the understanding of origin and evolution of granitic magmas", Geol. Rdsch., v. 76, p. 41-50.

Eberz, G.W. and Nicholls, I.A., 1990. "Chemical modification of enclave magma by post-emplacement crystal fractionation, diffusion and metasomatism", Contrib. Mineral. Petrol., v.104, p. 47-55.

Göncüoğlu, C.M., Turhan, N., Şentürk, K., Uysal, Ş., Özcan, A. and Işık, A., 1992. "The real location of the İzmir-Ankara suture: structural relationship between Anatolides and Pontides in the middle Sakarya region", I.S.G.B Abstracts.

Göncüoğlu, C.M., 1997, "Distribution of Lower Paleozoic Units in the Alpine Terranes of Turkey:paleogeographic constraints. In: Göncüoğlu, M.C. & Derman, A.S. (eds) Lower Paleozoic Evolution in Northwest Gondwana", Turkish Association of Petroleum Geologists, Special Publications, v.3, p.13-24.

Göncüoğlu, C.M., Turhan, N., Şentürk, K., Özcan, A., Uysal, Ş. and Yalınız, M.K., 2000. "A geotraverse across Northwestern Turkey: tectonic units of the Central Sakarya region and their tectonic evolution", Geological Society of London, Special Publicaitons, v.173, p. 139-161.

Harker, A., 1909. The natural history of igneous rocks, MacMillan, New York.

Helvacı, C. ve Bozkurt, S., 1991. "Beypazarı (Ankara) granitinin jeolojisi, mineralojisi ve petrojenezi", TJK abstracts.

Helvacı, C. and Bozkurt, S., 1994. "Geology, mineralogy and petrogenesis of Beypazarı (Ankara) granite", Geological Bulletin of Turkey, V.37, No. 2, p. 31-42.

Helvacı, C. and Yağmurlu, F., 1994. "Sedimentological characteristics and facies of the evaporite-bearing Kirmir Formation (Neogene), Beypazarı Basin, central Anatolia, Turkey", Sedimentology, v.41, p. 847-860.

Kalafatçıoğlu, A. and Uysallı, H., 1964. "Geology of the Beypazarı-Nallıhan-Seben Region", Bull. MTA, v. 62, p.1-11.

Karadenizli, L., 1995. "Sedimentology of the Upper Miocene-Pliocene gypsium series of the Beypazarı Basin, west of Ankara, Central Anatolia, Turkey", Geological Bulletin of Turkey, V.38, No. 1, p. 63-74

Kayakıran, S. ve Çelik, E., (1986). "Beypazarı trona yatağı maden jeolojisi raporu cilt I", MTA, Rep. No. 8079 (unpublished).

Kerr, P.F., 1959. Optical Mineralogy, Mc Graw Hill, New York.

Koçyiğit, A., 1987. "Tectono-stratigraphy of the Hasanoğlan (Ankara) Region: Evolution of the Karakaya Orogen", Yerbilimleri, v. 14, p. 269-293.

Koçyiğit, A., Altıner, D., Farinacci, A., Nicosia, U. and Conti, M.A., 1991. "Late Triassic- Aptian Evolution of the Sakarya Divergent Margin: implication for the opening history of the northern Neo-Tethys, in the north-western Anatolia, Turkey", Geologica Romana, v. 27, p. 81-99.

Koçyiğit, A., Winchester, J.A., Bozkurt, E., Holland, G., 2003. "Saraçköy Volcanic Suite: implications for the subductional phase of arc evolution in the Galatean Arc Complex, Ankara, Turkey", Geological Journal, v. 38, p. 1-14.

Maniar, P.D. and Piccoli, P.M., 1989. "Tectonic discrimination of granitods", Geological Society of America Bulletin, v.101, p. 635-643.

Mc Birney, A.R. and Noyes, R., 1979. "Crystallization and layering of the Skaergard intrusion", Journal of Petrology, v. 20, p. 185-212.

MTA, 2002. 1:500.000 scale geological maps of Turkey, No:2, 8.

Özçelik, O., 2002. "Organic geochemical characteristics of Miocene bituminous units, north of Beypazarı (Ankara)", Geological Bulletin of Turkey, V.45, No. 1, p. 1-15.

Peacock, M.A., 1931, Classification of igneous rock series, Journal of Geology, vol.39, p.54-67.

Pearce, J.A., Harris, N. B. W. and Tindle, A.G., 1984. "Trace element discrimination diagrams for the tectonic interpretation of Granitic Rocks", Journal of Petrology, v.25, p. 956-983.

Poli, G.E., and Tommasini, S., 1991. "Model for the origin and significance enclaves in calc-alkaline granitoids", Journal of Petrology, v.32, p. 657-666.

Raymond, L.A., 2001. Petrology: the Study of Igneous, Sedimentary, Metamorphic Rocks, WCB, USA.

Shand, S.J., 1951. Eruptive rocks, John Wiley, New York.

Streckeisen, A., 1976, "To each plutonic rock its proper name", Earth Science Review, v.12, p. 1-33.

Şengör, A.M.C. and Yılmaz, Y., 1981. "Tethyan evolution of Turkey: A plate tectonic approach", Tectonophysics, v.75, p.181-241.

Taylor, S.R. and Mc Lennon, S.N., 1985. "The continental crust: Its composition and evolution", Oxford: Blackwell Scientific Publishers.

Van Der Meer Mohr, 1956. "Beypazarı bölgesinde jeolojik ve hidrojeolojik saha çalışmalar hakkında Rapor", MTA, Rep. No. 2554 (Unpublished).

Vernon, R.H., 1986. "K-feldspar megacrysts in granites — phenocrysts, not porphyroblasts", Earth-Science Reviews, v.23, p.1-63.

Weingart, 1954. "56/2, 56/4 Sivrihisar ve 57/1, 57/3 Ankara petrografisi ve microsedimanter paftalarının jeolojik haritası hakkında rapor", MTA, Rap. No. 2248 (Unpublished).

White, A.J.R. and Chappell, B.W., 1977. "Ultrametamorphism and granitoid genesis", Tectonophysics, v.43, p. 7-22.

White, A.J.R., 1979. "Source of granite magmas", Geol. Soc. Am. Ann. Gen. Meeting, 539.

Winchester, J. A. and Floyd, P. A., 1977. "Geochemical discrimination of different magma series and their differentiation products using immobile elements", Chemical Geology, v.20, p.325-343.

Yağmurlu, F., Helvacı, C., İnci, U. and Önal, M., 1988. "Tectonic characteristics and structural evolution of the Beypazarı and Nallıhan Neogene basin, central Anatolia", Metu Journal of Pure and Applied sciences, v. 21, 1-3, 127-143.

Yılmaz, Y., 1981. "Sakarya kıtası güney kenarının evrimi", İstanbul University Earth Sciences, v. ½, 33-52.

Yohannes, E., 1993. "Geology and Petrology of the Beypazarı Granitoids", M.S thesis in Graduate School of Natural and Applied Sciences, Geological Engineering Department, Middle East Technical University, Ankara.